Competition between pattern reconstruction and sequence processing in nonsymmetric neural networks



1992 J. Phys. A: Math. Gen. 25 5493

(http://iopscience.iop.org/0305-4470/25/21/011)

J. Phys. A: Math. Gen. 25 (1992) 5493–5526. Printed in the UK

# Competition between pattern reconstruction and sequence processing in non-symmetric neural networks

A C C Coolen and D Sherrington

Department of Physics, Theoretical Physics, University of Oxford, 1 Keble Road, Oxford OX1 3NP, UK

Received 14 May 1992

**Abstract.** We study an Ising spin neural network model in which the interaction matrix consists of a symmetric Hebbian term (which favours the reconstruction of static patterns) and a non-symmetric transition term (which favours limit cycles corresponding to the processing of pattern sequences). We calculate phase diagrams and analyse the relation between the relative weight of the two competing contributions to the interaction matrix and the frequency of the periodic attractors.

## 1. Introduction

Ising spin models for neural networks have made a significant contribution to our understanding of parallel information processing in nervous tissue. Following the pioneering work by Little [1], Hopfield [2] and Amit *et al* [3] many such models have been constructed and analysed. Representing the states of neurons as binary variables, which evolve in time according to a stochastic local field alignment, may be a crude simplification of biological reality. On the other hand it often allows for a detailed quantitative analysis. Choosing simple neural variables $\{s_i\}$ enables one to choose more complicated synaptic interaction matrices $\{J_{ij}\}$, and *vice versa*. A common feature of most statistical mechanical models for neural networks is the *separability* of the interaction matrix, which naturally leads to a convenient description in terms of macroscopic order parameters. A second important property shared by many models is the symmetry of the interaction matrix. If $J$ is symmetric, then the stochastic local field alignment obeys detailed balance and one can immediately apply equilibrium statistical mechanics. The system's phase diagram can be understood in terms of the minimization of some scalar quantitity (in equilibrium to be identified with the free energy). The system will always evolve to some equilibrium configuration, even if in the thermodynamic limit ergodicity is broken. If, on the other hand, the interaction matrix is not symmetric, then the microscopic probability distribution will again evolve in time to some equilibrium solution; detailed balance, however, no longer holds. In the case of ergodicity breaking in the thermodynamic limit (i.e on finite timescales) the system might end up in limit cycles or even in chaotic trajectories. It will no longer be possible to apply equilibrium statistical mechanics or to think in terms of some scalar quantity being minimized. One must study the dynamics directly, as in [4].

0305-4470/92/215493+34$07.50  

In this paper we analyse an Ising spin neural network model (of $N$ spins) in which the interaction matrix consists of two terms: a (symmetric) Hebbian [5] term, which tends to stabilize a given set of $p$ patterns, and a (non-symmetric) transition term, which tends to create period-$p$ limit cycles (or sequences) composed of the same set of $p$ patterns. Clearly there will be a competition between the two tendencies, controlled by the relative weight $\nu$ of the two competing terms. There are several motivations for studying this particular model. The first motivation is that competition between incompatible physical processes usually leads to interesting phenomena (the Hopfield model itself is, in fact, based on competition between fixed-point attractors); nice recent examples in the context of neural network models are the papers by Dotsenko [6] (competition between the Hebb [5] matrix and the pseudo-inverse [7] matrix) and by Evans *et al* [8] (competition between the Hebb matrix and a symmetry transformation term, in order to achieve invariant pattern recognition). In both of these examples, however, the competition is between two *symmetric* matrix contributions, whereas the present model involves competition between a symmetric term and a non-symmetric term (i.e. competition between fixed-point attractors and non-stationary limit cycles). The second motivation for studying the present model is that it arises naturally in the context of modelling chemical modulation in neural systems [9]. If during a Hebbian [5] learning phase both static patterns and sequences of patterns are presented to a network with transmission delays, then this network will develop interactions which are a combination of a Hebbian term and a transition term. Furthermore, due to the incorporation into the model of chemical modulators (as in [10]), the relative weight of the two terms will be a function of the actual chemical setting in the recall phase. Consequently, studying the effect of neuromodulators on the information-processing properties of such a model implies studying the physics of the present model as a function of the relative weight $\nu$ of the two terms in the interaction matrix. The third motivation for studying the present model presented itself *a posteriori* when reading the recent papers by Griniasty *et al* [11] and Cugliandolo [12]. These authors show that experiments on monkeys by Miyashita *et al* [13], which demonstrate that sequentially learned stimuli of uncorrelated patterns can produce correlated attractors, can be explained by Ising spin models in which the interaction matrix is exactly the symmetric part of the matrix in our model. Since the authors seem to have put in the symmetry of their interaction matrix to simplify the analysis, the present model can be seen as a natural next step in explaining the aforementioned physiological data. Finally, we would like to emphasize that, in general, non-symmetric models built around transition matrices (constructed for explaining temporal association in nervous tissue) are far less intensively studied than symmetric attractor models. A nice overview of the theory developed in this field (until 1990) can be found in [14]. In particular, the model studied in the present paper can be seen as the zero delay limit of the one introduced by Sompolinsky and Kanter [15]. Only recently have some authors tried to go beyond simulation studies and the analysis of some specific types of dynamic solutions to the macroscopic equations, and to perform a more thorough mathematical analysis of the physics contained in such models [16–18].

This paper is organized as follows. In section 2 we define our model and the two types of stochastic local field alignment considered (sequential and parallel) and derive the corresponding macroscopic evolution laws for the order parameters (restricting ourselves to the case $p \ll \sqrt{N}$) in the thermodynamic limit $N \to \infty$. We solve the case $p = 2$ directly (which is a trivial case in the sense that the order parameters decouple). In sections 2 and 3 we analyse the types of fixed-points possible in terms

of a $T/\nu$ phase diagram (where $T$ is the temperature) and their stability properties. Apart from a second-order phase transition we show that for $p > 2$ there is also a first-order transition. In section 5 we exploit symmetries of the pattern distribution, which enables us to explain for parallel dynamics a symmetry of the phase diagram and to show that all dynamic solutions of the macroscopic equations in the region $\nu > \frac{1}{2}$ (where the Hebbian term is the more important one) are related to the solutions in the region $\nu < \frac{1}{2}$ (where the transition term is the more important one) by a time-dependent unitary transformation. Finally in section 6 we present results of numerical iteration of the macroscopic laws and we analyse, for parallel dynamics, the relation between the relative weight $\nu$ of the two contributions to the synaptic matrix and the frequency of the periodic attractors.

## 2. Model definitions and evolution of order parameters

### 2.1. *Model definitions*

Our model will be an Ising spin neural network of $N$ spins $s_i \in \{-1, 1\}$. If neuron $i$ is at rest we put $s_i = -1$; if neuron $i$ is firing we put $s_i = 1$. We will study a system that has learned a given set $\{\xi^\mu\}$ $(\mu = 1 \ldots p)$ of patterns $\xi^\mu \in \{-1, 1\}^N$. If the learning stage consisted of two Hebbian [5] phases, a first one during which the patterns were learned as static objects and a second one during which the patterns were learned as dynamic objects, the final connection matrix (representing the synaptic interactions between the neurons) will be

$$J_{ij} = \frac{\nu}{N} \sum_\mu \xi_i^\mu \xi_j^\mu + \frac{1-\nu}{N} \sum_\mu \xi_i^{\mu+1} \xi_j^\mu \qquad (\mu : \text{ mod } p)$$

or

$$J_{ij} = \frac{1}{N} \sum_{\mu\rho} \xi_i^\mu A_{\mu\rho} \xi_j^\rho \tag{1}$$

$$A_{\mu\rho} \equiv \nu \delta_{\mu\rho} + (1-\nu) S_{\mu\rho} \qquad S_{\mu\rho} \equiv \delta_{\mu,\rho+1} \qquad (\mu : \text{ mod } p). \tag{2}$$

If we define $0 \leqslant \nu \leqslant 1$ the parameter $\nu$ will enable us to interpolate smoothly between the familiar and analytically well understood Hopfield [2] model ($\nu = 1$) and the far less intensively studied sequence processing model ($\nu = 0$).

We will consider two types of rules for the evolution in time of the microscopic state probability $p_t(s)$, both based on stochastic local field alignment with the local fields as given by (3)

$$h_i = \sum_{j=1}^N J_{ij} s_j. \tag{3}$$

First we will take time to be a continuous variable and define the evolution in time of $p_t(s)$ by the master equation:

$$\frac{\mathrm{d}}{\mathrm{d}t} p_t(s) = \sum_{j=1}^N p_t(F_j s) w_j(F_j s) - \sum_{j=1}^N p_t(s) w_j(s) \tag{4}$$

where $F_j$ is the spin-flip operator, i.e. $F_j\Phi(s_1,\ldots,s_N)\equiv\Phi(s_1,\ldots,-s_j,\ldots,s_N)$, and the transition rates $w_j(s)$ are defined as

$$w_j(s)\equiv\tfrac{1}{2}[1-\tanh(\beta s_j h_j)].$$

The second type of dynamics considered is a parallel stochastic local field alignment in the form of a Markov process; now time is a discrete variable:

$$p_{t+1}(s)\equiv\sum_{s'}w(s'\to s)p_t(s'). \tag{5}$$

The transition probabilities $w(s'\to s)$ are defined as

$$w(s'\to s)\equiv\prod_{j=1}^{N}\tfrac{1}{2}[1+s_j\tanh(\beta h_j')].$$

Since for $p>2$ the interaction matrix (1) is non-symmetric one cannot define a Hamiltonian such that the stochastic local field alignment becomes a Glauber dynamics; therefore equilibrium statistical mechanics is not applicable. In order to analyse the system's dynamics we will introduce $p$ macroscopic quantities for describing a given macroscopic state $s$:

$$q_\mu(s)\equiv\frac{1}{N}\sum_{i=1}^{N}\xi_i^\mu s_i \qquad (\mu=1\ldots p).$$

In terms of these macroscopic variables we can now write the local fields $h_i$ as

$$h_i=\xi_i\cdot Aq(s).$$

Throughout this paper we will assume $p$ (the number of patterns stored) to obey $p\ll\sqrt{N}$.

### 2.2. *The macroscopic laws*

Following the derivations in [4] and [19] we find the evolution in time of the macroscopic quantities $q$ to become deterministic in the thermodynamic limit $N\to\infty$. For case (4) the evolution in time is governed by the set of coupled nonlinear differential equations:

$$\frac{\mathrm{d}}{\mathrm{d}t}q=\lim_{N\to\infty}\frac{1}{N}\sum_{i=1}^{N}\xi_i\tanh[\beta\xi_i\cdot Aq]-q \tag{6}$$

where $\xi_i\equiv(\xi_i^1,..,\xi_i^p)\in\{-1,1\}^p$. For the case of a parallel Markov process (5) one finds a set of coupled nonlinear mappings [20]:

$$q(t+1)=\lim_{N\to\infty}\frac{1}{N}\sum_{i=1}^{N}\xi_i\tanh[\beta\xi_i\cdot Aq(t)]. \tag{7}$$

If, furthermore, the pattern components $\xi_i^\mu$ are drawn at random from $\{-1, 1\}$, we find in the thermodynamic limit equation (6) being replaced by (8) and equation (7) being replaced by (9):

$$\frac{\mathrm{d}}{\mathrm{d}t}q = \langle \xi \tanh[\beta \xi \cdot Aq] \rangle_\xi - q \tag{8}$$

$$q(t+1) = \langle \xi \tanh[\beta \xi \cdot Aq(t)] \rangle_\xi \tag{9}$$

where the average is defined as

$$\langle \Phi(\xi) \rangle_\xi \equiv 2^{-p} \sum_{\xi \in \{-1,1\}^p} \Phi(\xi).$$

For future use we will briefly indicate some of the properties of the matrices encountered. For the index permutation matrix $S$ (2) one finds

$$S^\dagger S = S S^\dagger = 1 \qquad S^p = 1.$$

Since the Hermitian part $\frac{1}{2}(A + A^\dagger)$ and the anti-Hermitian part $\frac{1}{2}(A - A^\dagger)$ of the matrix $A$ (2) commute, it must have a complete set of orthogonal eigenvectors $\{|n\rangle\}$. This set turns out to be

$$|n\rangle \equiv (\hat{e}_1^n, \ldots, \hat{e}_p^n) \qquad n = 0, \ldots, p-1$$

$$\hat{e}_\lambda^n \equiv \frac{1}{\sqrt{p}} \mathrm{e}^{2\pi \mathrm{i} n \lambda / p}. \tag{10}$$

One can easily show that the following relations hold:

$$\langle n|m\rangle \equiv \sum_{\lambda=1}^{p} \hat{e}_\lambda^{n*} \hat{e}_\lambda^m = \delta_{nm}$$

$$S|n\rangle = \mathrm{e}^{-2\pi \mathrm{i} n/p}|n\rangle \qquad S^\dagger|n\rangle = \mathrm{e}^{2\pi \mathrm{i} n/p}|n\rangle \tag{11}$$

$$A|n\rangle = \left[\nu + (1-\nu)\mathrm{e}^{-2\pi \mathrm{i} n/p}\right]|n\rangle \equiv a_n|n\rangle.$$

In a subsequent section we will also encounter the index permutation matrix $K$:

$$K_{\lambda\rho} \equiv \delta_{\lambda, p+1-\rho} \qquad (\lambda, \rho : \mod p)$$

for which

$$K = K^\dagger \qquad K^2 = 1 \qquad KSK = S^\dagger \qquad KS^\dagger K = S$$

$$K|n\rangle = \mathrm{e}^{2\pi \mathrm{i} n/p}|p-n\rangle.$$

### 2.3. *A toy problem: the symmetric case* $p = 2$

Solution of the model becomes straightforward if $p = 2$. Now there are only two order parameters, which decouple. Since $p = 2$ is exactly the situation where the interaction matrix $\{J_{ij}\}$ is symmetric, one can perform a thermodynamic analysis.

Upon introduction of the variables $z^{\pm} \equiv q_1 \pm q_2$, one finds, after performing the pattern averages involved, that both dynamic laws (8) and (9) decouple into independent one-dimensional evolution laws. In the case of sequential dynamics one obtains in terms of the new variables:

$$\frac{\mathrm{d}}{\mathrm{d}t}z^{+} = \tanh[\beta z^{+}] - z^{+} \qquad \frac{\mathrm{d}}{\mathrm{d}t}z^{-} = \tanh[\beta(2\nu-1)z^{-}] - z^{-} \tag{12}$$

whereas in the case of parallel dynamics one obtains in terms of $z^{\pm}$:

$$z^{+}_{t+1} = \tanh[\beta z^{+}_{t}] \qquad z^{-}_{t+1} = \tanh[\beta(2\nu-1)z^{-}_{t}]. \tag{13}$$

If we now define $m[\beta]$ as the non-negative solution of the transcendental equation $m = \tanh[\beta m]$ we can describe the asymptotic behaviour of (12) and (13) as follows:

*Sequential dynamics*

$1 < T$: $\quad z^{\pm}_{t} \to 0 \qquad (t \to \infty)$

$2\nu - 1 < T < 1$: $\quad z^{+}_{t} \to \mathrm{sign}[z^{+}_{0}]m[\beta]$, $\; z^{-}_{t} \to 0 \qquad (t \to \infty)$

$0 < T < 2\nu - 1$: $\quad z^{+}_{t} \to \mathrm{sign}[z^{+}_{0}]m[\beta]$, $\; z^{-}_{t} \to \mathrm{sign}[z^{-}_{0}]m[\beta(2\nu-1)] \qquad (t \to \infty).$

*Parallel dynamics*

$1 < T$: $\quad z^{\pm}_{t} \to 0 \qquad (t \to \infty)$

$|2\nu - 1| < T < 1$: $\quad z^{+}_{t} \to \mathrm{sign}[z^{+}_{0}]m[\beta]$, $\; z^{-}_{t} \to 0 \qquad (t \to \infty)$

$0 < T < 2\nu - 1$: $\quad z^{+}_{t} \to \mathrm{sign}[z^{+}_{0}]m[\beta]$, $\; z^{-}_{t} \to \mathrm{sign}[z^{-}_{0}]m[\beta(2\nu-1)] \qquad (t \to \infty)$

$0 < T < 1 - 2\nu$: $\quad z^{+}_{t} \to \mathrm{sign}[z^{+}_{0}]m[\beta]$, $\; z^{-}_{t} \to (-1)^{t}\,\mathrm{sign}[z^{-}_{0}]m[\beta(1-2\nu)] \qquad (t \to \infty).$

In the case of sequential dynamics we may conclude that there are two second-order phase transitions at the lines $T = 1$ (where the system goes from the paramagnetic state to an ordered state which is equally correlated with the two patterns) and at $T = 2\nu - 1$ (where the system enters the region in which the two patterns can be distinguished). Both transitions correspond to continuous bifurcations of new fixed-points. The system will always approach an equilibrium configuration (as it should be). In the case of parallel dynamics there are three continuous transitions: at the line $T = 1$ (where the system goes from the paramagnetic state to an ordered state which is equally correlated with the two patterns), at $T = 2\nu - 1$ (where the system

enters the region in which the patterns can be distinguished) and at $T = 1 - 2\nu$ (where there is a transition from the region of the equally correlated fixed-point to that where the system will flow towards a period-2 limit cycle), with a triple point at $(T,\nu) = (0,\frac{1}{2})$. The transitions at $T = 1$ and $T = 2\nu - 1$ are again ordinary second-order transitions, indicating the continuous bifurcation of a new fixed-point. The transition at $T = 1 - 2\nu$ is of a different type (the system goes from a fixed-point into a limit cycle).

The alternative approach (only applicable in the present case $p = 2$) is to perform a standard thermodynamic analysis. The symmetry of the interaction matrix allows us to conclude (after elimination of the diagonal elements $J_{ii}$) that for the sequential evolution in time (4) the equilibrium probability distribution is the Gibbs distribution, with the Hamiltonian $H$:

$$p_\infty(s) \sim \mathrm{e}^{-\beta H} \qquad H = -\tfrac{1}{2}\sum_{i\neq j} s_i J_{ij} s_j .$$

Using the standard procedures [3] one can now calculate the free energy per spin $f[\beta] \equiv -(1/\beta N)\log \mathcal{Z}_N[\beta]$ in the thermodynamic limit $N \to \infty$ (for $p$ fixed). Introduction of the auxiliary variables $z_\pm \equiv q_1 \pm q_2$ leads to a factorization of the partition function $\mathcal{Z}_N[\beta]$, in which the summation over all possible spin states decouples into independent summations over the spin states in disconnected sublattices $I_\pm$:

$$I_\pm \equiv \{i = 1,\ldots,N \mid \xi_i^1 = \pm\xi_i^2\}.$$

The final result is

$$\lim_{N\to\infty} f[\beta] = -\frac{1}{\beta}\log 2 + \frac{1}{2}\left\{\frac{1}{2}z_+^2 - \frac{1}{\beta}\log\cosh[\beta z_+]\right\} + \frac{1}{2}\left\{\frac{1}{2}(2\nu-1)z_-^2 - \frac{1}{\beta}\log\cosh[\beta(2\nu-1)z_-]\right\} \tag{14}$$

where the order parameters $z_\pm \equiv q_1 \pm q_2$ are those solutions of

$$z_+ = \tanh[\beta z_+] \qquad z_- = \tanh[\beta(2\nu-1)z_-]$$

that minimize expression (14). We can now understand the dynamics of the order parameters in terms of free energy minimization. The ground-state energy per spin $E_0$ is obtained by taking the limit $\beta \to \infty$ in (14), with the result $E_0 = -\frac{1}{4}$ (for $\nu \leqslant \frac{1}{2}$) and $E_0 = -\frac{1}{2}\nu$ (for $\nu > \frac{1}{2}$).

In the case of parallel dynamics (5) it has been shown [21] that the equilibrium probability distribution is now given by

$$p_\infty(s) \sim \mathrm{e}^{-\beta\tilde{H}} \qquad \tilde{H} \equiv -\frac{1}{\beta}\sum_i \log\left[2\cosh\left(\beta\sum_j J_{ij}s_j\right)\right].$$

Using the above expression we can now again calculate the free energy per spin $\tilde{f}[\beta] \equiv -(1/\beta N)\log\tilde{\mathcal{Z}}_N[\beta]$ in the thermodynamic limit $N \to \infty$ (for $p$ fixed). Introduction of the auxiliary variables $z_\pm \equiv q_1 \pm q_2$ again leads to a factorization of the partition function $\tilde{\mathcal{Z}}_N[\beta]$, in which the summation over all possible spin states

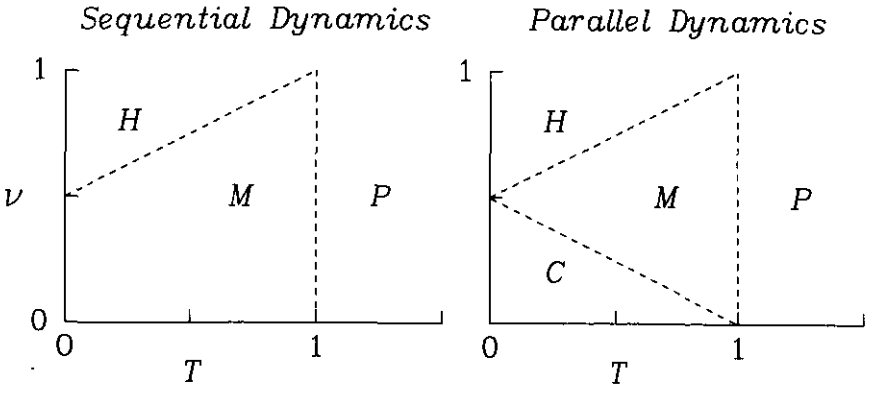


**Figure 1.** The $p = 2$ phase diagrams: $P$, paramagnetic region, $q = 0$: $M$, mixture region, $q \neq 0$, $q_1 = q_2$; $H$, Hopfield region, $q \neq 0$, $q_1 \neq q_2$; $C$, cycle region, $q(t+2) = q(t)$, $q(t+1) \neq q(t)$.

decouples into independent summations over the spin states in the disconnected sublattices $I_\pm$. The final result takes the form:

$$\lim_{N\to\infty} \tilde{f}[\beta] = -\frac{2}{\beta}\log 2 + \frac{1}{2\beta}\min_{z_+}\{c^*(z_+) - \log\cosh[\beta z_+]\}$$
$$+ \frac{1}{2\beta}\min_{z_-}\{c^*(z_-) - \log\cosh[\beta(2\nu-1)z_-]\}$$

$$c^*(m) \equiv \tfrac{1}{2}(1+m)\log(1+m) + \tfrac{1}{2}(1-m)\log(1-m).$$

The saddle points are the solutions of

$$z_+ = \tanh\left[\beta\tanh\left[\beta z_+\right]\right] \qquad z_- = \tanh\left[\beta(2\nu-1)\tanh\left[\beta(2\nu-1)z_-\right]\right].$$

From which one can, in turn, again deduce that

$$z_+ = \tanh\left[\beta z_+\right] \qquad z_- = \tanh\left[\beta(2\nu-1)z_-\right].$$

Therefore the final expression for the free energy per spin becomes

$$\lim_{N\to\infty} \tilde{f}[\beta] = -\frac{1}{\beta}2\log 2 + \frac{1}{2}z_+^2 - \frac{1}{\beta}\log\cosh[\beta z_+]$$
$$+ \frac{1}{2}(2\nu-1)z_-^2 - \frac{1}{\beta}\log\cosh[\beta(2\nu-1)z_-] \tag{15}$$

in which the order parameters $z_\pm \equiv q_1 \pm q_2$ are those solutions of the saddle-point equations that minimize expression (15). We can now understand the evolution of order parameters for parallel dynamics again in terms of free energy minimization. As was the case for the Hopfield model [3] the free energy for parallel dynamics is exactly twice the free energy obtained for sequential dynamics. The important difference with having sequential dynamics, of course, is the presence of period-2 limit cycles, which are the consequence of the fact that for parallel dynamics only one iteration step is sufficient to perform the state change $z_- \to -z_-$ (which is energetically allowed).

The $p = 2$ phase diagrams obtained in this section are shown in figure 1.

## 3. Fixed-points

### *3.1. Critical temperature*

The fixed-point solutions of (8) and (9) follow from the corresponding fixed-point equation:

$$q = \langle \xi \tanh(\beta \xi \cdot Aq) \rangle_\xi . \tag{16}$$

We will first calculate the critical temperature $T_c \equiv \beta_c^{-1}$ for the existence of non-trivial solutions of the fixed-point equation. For a non-trivial solution $q \neq 0$ of (16) we find that

$$\begin{aligned} q^2 = q \cdot \left\{ \left\langle \xi(\xi \cdot Aq)\beta \int_0^1 d\lambda \left[1 - \tanh^2(\beta\lambda\xi \cdot Aq)\right] \right\rangle_\xi \right\} \\ = \tfrac{1}{2}\beta \langle \left\{ (\xi \cdot q)^2 + (\xi \cdot Aq)^2 - [\xi \cdot (1 - A)q]^2 \right\} \\ \times \int_0^1 d\lambda \left[1 - \tanh^2(\beta\lambda\xi \cdot Aq)\right] \rangle_\xi \leqslant \tfrac{1}{2}\beta \left\{ \langle (\xi \cdot q)^2 \rangle_\xi + \langle (\xi \cdot Aq)^2 \rangle_\xi \right\} \\ = \frac{1}{2}\beta q^2 \left\{ 1 + \frac{q \cdot A^\dagger Aq}{q^2} \right\} \end{aligned}$$

which for $q \neq 0$ implies (with $T \equiv \beta^{-1}$):

$$T \leqslant \frac{1}{2} \left\{ 1 + \max_q \frac{q \cdot A^\dagger Aq}{q^2} \right\} .$$

In deriving this inequality we have used the statistical independence of the stored patterns: $\langle \xi_\mu \xi_\nu \rangle = \delta_{\mu\nu}$. Since for the matrix $A$ at hand (2) there exists a complete orthonormal basis $\{|n\rangle\}$ of eigenvectors (10) we may write

$$T \leqslant \tfrac{1}{2} + \tfrac{1}{2} \max_n \langle n|A^\dagger A|n\rangle = \tfrac{1}{2} + \tfrac{1}{2} \max_n \left| \nu + (1 - \nu)e^{-2\pi i n/p} \right|^2 = 1 .$$

Since for $T < 1$ non-trivial fixed-points do exist (as we will see), the critical temperature (as far as fixed-points are concerned) is clearly $T_c = 1$.

Next we want to find out how, for $T < 1$, non-trivial solutions of the fixed-point equation (16) bifurcate. If we differentiate both sides of (16) with respect to either $\beta$ or $\nu$ we obtain

$$[1 - \beta\Gamma(q)A] \frac{\partial q}{\partial \beta} = \Gamma(q)Aq$$

$$[1 - \beta\Gamma(q)A] \frac{\partial q}{\partial \nu} = \beta\Gamma(q) \frac{\partial A}{\partial \nu} q$$

where the matrix $\Gamma(q)$ is defined as

$$\Gamma(q)_{\lambda\rho} \equiv \langle \xi_\lambda \xi_\rho \left[1 - \tanh^2(\beta \xi \cdot Aq)\right] \rangle_\xi . \tag{17}$$

As a bifurcation parameter one can either take $\beta$ or $\nu$. Taking $\beta$ as a bifurcation parameter a fixed-point bifurcation occurs as soon as $\partial_\beta q$ is not uniquely defined; if we take $\nu$ as a bifurcation parameter we find a bifurcation if $\partial_\nu q$ is not uniquely defined. In both cases the condition for a new solution of (16) to bifurcate is

$$\det |1 - \beta\Gamma(q)A| = 0 . \tag{18}$$

Equations (16) and (18) are to be solved simultaneously.

*3.2. Continuous bifurcations from the trivial fixed-point*

Since for $T > 1$ the only fixed-point is $q = 0$, we will first consider continuous bifurcations from this trivial fixed-point. Since $\Gamma(\mathbf{0})_{\lambda\rho} = \delta_{\lambda\rho}$ equation (18) turns into $\det|1 - \beta A| = 0$ or

$$\exists|x\rangle : A|x\rangle = T|x\rangle.$$

In terms of the basis $\{|n\rangle\}$ (10) of eigenvectors of $A$ this implies

$$\langle n|x\rangle \left[\nu + (1-\nu)e^{2\pi i n/p} - T\right] = 0 \qquad n = 0, \ldots, p-1. \tag{19}$$

If $\nu = 1$ we are in fact studying the Hopfield model [2]: $A$ reduces to the identity matrix and we need higher order expansions for determining which types of fixed-points bifurcate at $T = 1$ (which turn out to be the well known pure and mixture states). However, for $\nu < 1$ the fixed-point equation (16) is far more restrictive with regard to the types of fixed-points allowed. If $p$ is odd there is only one solution for the above set of equations (19): $|x\rangle = |0\rangle = (1/\sqrt{p})(1, \ldots, 1)$ (with corresponding bifurcation temperature $T_b = 1$); if $p$ is even and $\nu > \frac{1}{2}$ there is also the solution $|x\rangle = |p/2\rangle = (1/\sqrt{p})(1, -1, \ldots, 1, -1)$ (with bifurcation temperature $T_b = 2\nu - 1$). These solutions correspond to full even mixtures of all stored patterns and alternating full mixtures of all stored patterns, respectively, and turn out to constitute solutions of the fixed-point equation (16) for any $T$:

$$q^+ \equiv q^+[\beta]|0\rangle \tag{20}$$

$$q^- \equiv q^-[\beta]|p/2\rangle \tag{21}$$

where the amplitudes $q^+[\beta]$ and $q^-[\beta]$ are the non-trivial solutions of

$$q^+ = \sqrt{p}\langle m \tanh[\beta q^+ m\sqrt{p}]\rangle \tag{22}$$

$$q^- = \sqrt{p}\langle m \tanh[\beta(2\nu - 1)q^- m\sqrt{p}]\rangle \tag{23}$$

where $m \equiv (1/p)\sum_{\rho=1}^{p} \xi_\rho$. The existence of the non-trivial fixed-point $q^+$ for $T < 1$ confirms our previous statement that the critical temperature for fixed-points is indeed $T_c = 1$. Note that the alternating mixture exists only if $p$ is even and $T < 2\nu - 1$, and that in the latter case the two amplitudes are related by $q^-[\beta] = q^+[\beta(2\nu - 1)]$.

*3.3. Continuous bifurcations from the symmetric fixed-points*

The next step is to find out whether for $T < 1$ there exist fixed-point solutions that, in turn, bifurcate continuously from either the mixture state $q^+$ or (for $p$ even and $T < 2\nu - 1$) from $q^-$. Since both $q^+$ and $q^-$ are solutions of (16), we can find the continuously bifurcating fixed-points by solving

$$\det|1 - \beta\Gamma(q^\pm)A| = 0$$

in which

$$\begin{aligned} \Gamma(q^+) &= D^+[\beta] + R^+[\beta]|0\rangle\langle 0| \\ \Gamma(q^-) &= D^-[\beta] + R^-[\beta]|p/2\rangle\langle p/2| \end{aligned} \tag{24}$$

and

$$D^+[\beta] = \frac{p}{p-1}\left\langle [1-m^2]\,[1-\tanh^2(\beta q^+[\beta] m\sqrt{p})]\right\rangle$$

$$R^+[\beta] = \frac{p}{p-1}\left\langle [pm^2-1]\,[1-\tanh^2(\beta q^+[\beta] m\sqrt{p})]\right\rangle$$

$$D^-[\beta] = D^+[\beta(2\nu-1)] \qquad R^-[\beta] = R^+[\beta(2\nu-1)].$$

Having calculated the matrices $\Gamma(q^\pm)$ we can now solve (18). First we consider the bifurcations from $q^+$:

$$\exists|x\rangle : \{D^+[\beta] + R^+[\beta]|0\rangle\langle 0|\}\, A|x\rangle = T|x\rangle.$$

In terms of the basis $\{|n\rangle\}$ of eigenvectors of $A$ this implies:

$$\{D^+[\beta] + R^+[\beta]\delta_{n0}\}\left\{\nu + (1-\nu)e^{2\pi i n/p}\right\}\langle n|x\rangle = T\langle n|x\rangle \qquad n = 0,\ldots,p-1.$$

Therefore (since a bifurcation from $q^+$ cannot, by definition, be in the direction of $|0\rangle$):

$$\forall n \in \{1,..,p-1\} : \langle n|x\rangle = 0 \text{ or } T = D^+[\beta]\left\{\nu + (1-\nu)e^{2\pi i n/p}\right\}.$$

Since $T$ is a real quantity, there can be no continuous bifurcation from $q^+$ for odd $p$. For $p$ even the only possible continuous bifurcation from $q^+$ is in the direction of $|p/2\rangle$, with a corresponding bifurcation temperature determined by

$$1 = (2\nu-1)\beta_b D^+[\beta_b].$$

As might have been expected, the bifurcation temperature defined by this equation is below the critical temperatures for the existence of the two constituent fixed-point solutions.

In the same way one can analyse the continuous bifurcations (if present) from the alternating mixture state $q^-$ (for $p$ even and $T < 2\nu - 1$):

$$\exists|x\rangle : \{D^-[\beta] + R^-[\beta]|p/2\rangle\langle p/2|\}\, A|x\rangle = T|x\rangle.$$

In terms of the basis $\{|n\rangle\}$ of eigenvectors of $A$ this implies

$$\left\{D^-[\beta] + R^-[\beta]\delta_{n,p/2}\right\}\left\{\nu + (1-\nu)e^{2\pi i n/p}\right\}\langle n|x\rangle = T\langle n|x\rangle$$
$$n = 0,\ldots,p-1.$$

Therefore (since a bifurcation from $q^-$ cannot, by definition, be in the direction of $|p/2\rangle$):

$$\forall n \in \{1,..,p-1\} : \langle n|x\rangle = 0 \text{ or } T = D^-[\beta]\left\{\nu + (1-\nu)e^{2\pi i n/p}\right\}.$$

Since $T$ is a real quantity the only possible bifurcation from $q^-$ is in the direction of $|0\rangle$, with a corresponding bifurcation temperature given via

$$1 = \beta_b D^-[\beta_b].$$

### *3.4. Three regions in the $T/\nu$ phase diagram*

One can conclude from the above bifurcation analysis that for $T > 2\nu - 1$ only two non-trivial fixed-points can be found as the result of continuous bifurcations, namely $\pm q^+$ (20). In the appendix we prove that in the aforementioned regime the full mixture solutions $\pm q^+$ are, in fact, the *only* non-trivial fixed-points of equation (16) (which rules out the possibility of discontinuous bifurcations).

In the remaining regime $T \leqslant 2\nu - 1$ we have (for $p$ even) already encountered the fixed-points $\pm q^-$ (21) (the alternating mixtures). Since for $\nu = 1$ our model reduces to the Hopfield model [2], it is to be expected that there will also be fixed-point solutions related to the fixed-points of the Hopfield model. As soon as $\nu < 1$ we know that for $T > 0$ any non-trivial fixed-point $q \neq \mathbf{0}$ must have non-zero components $q_\mu \neq 0$ only, since from the fixed-point equation (16) one can deduce (with $\mathrm{sgn}[0] \equiv 0$):

$$\mathrm{sgn}[q_\mu] = \mathrm{sgn}[\nu q_\mu + (1-\nu)q_{\mu-1}] \qquad (\forall \mu, \bmod p)$$

($q_\mu = 0 \Rightarrow q_{\mu-1} = 0 \Rightarrow \cdots \Rightarrow q = \mathbf{0}$) Therefore, pure states and mixtures with only a finite number $n < p$ of non-zero components (as in the Hopfield model) cannot be fixed-points for $\nu < 1$ if $T > 0$. Only for $T = 0$ one can find for $\nu < 1$ non-trivial fixed-points with a finite number $n < p$ of non-zero components; pure states $q_\mu \equiv \delta_{\mu\rho}$, for instance, turn out to be fixed-points if $\nu > \frac{1}{2}$.

We will now make an expansion of the fixed-points in powers of $\eta \equiv 1 - \nu$. The zeroth order in this expansion will then precisely be a fixed-point of the Hopfield model, and subsequent orders will show how the fixed-points of the Hopfield model are modified as one tends away from the line $\nu = 1$ in the phase diagram:

$$\eta \equiv 1 - \nu: \qquad q \equiv \sum_{n \geqslant 0} q_n \eta^n \qquad A = 1 + \eta[S-1].$$

Insertion of the above expressions into the fixed-point equation (16) leads to recurrent relations for the expansion coefficients $q_n$:

$$q_0 = \langle \xi \tanh[\beta \xi \cdot q_0] \rangle_\xi$$

$$q_n = [1 - \beta\Gamma(q_0)]^{-1} \{\beta\Gamma(q_0)(S-1)q_{n-1} + \sum_{m=2}^{n} \frac{\beta^m}{m!} \sum_{k_1=1}^{n-m+1} \cdots \sum_{k_m=1}^{n-m+1} \delta_{n,k_1+\cdots+k_m} \langle \xi(\xi \cdot z_{k_1}) \cdots (\xi \cdot z_{k_m}) \tanh^{(m)}[\beta \xi \cdot q_0] \rangle\} \qquad (n \geqslant 1)$$

$$z_l \equiv q_l + [S-1]\, q_{l-1}$$

where the matrix $\Gamma$ is defined by (17). Each fixed-point $q_0$ of the Hopfield model thus generates a fixed-point $q$ for the present model (in the regime $T < 2\nu - 1$) in the form of a series expansion in powers of $1 - \nu$. Upon choosing for $q_0$ a pure state $q_0 \equiv q^*(1, 0, .., 0)$ one finds

$$q^* = \tanh[\beta q^*]$$

$$q_n = [1-\beta(1-q^{*2})]^{-1}\left\{\beta(1-q^{*2})(S-1)q_{n-1} + \sum_{m=2}^{n}\frac{\beta^m}{m!}\tanh^{(m)}[\beta q^*]\right.$$
$$\left.\times \sum_{k_1=1}^{n-m+1}\cdots\sum_{k_m=1}^{n-m+1}\delta_{n,k_1+\cdots+k_m}\langle\xi(\xi\cdot z_{k_1})\cdots(\xi\cdot z_{k_m})\xi_1^{m+1}\rangle_\xi\right\}$$

resulting in

$$q = q^*(1,0,\ldots,0) + (1-\nu)\frac{\beta q^*(1-q^{*2})}{1-\beta(1-q^{*2})}(-1,0,\ldots,0,1)$$
$$+ (1-\nu)^2\frac{\beta^2 q^*(1-q^{*2})}{[1-\beta(1-q^{*2})]^3}\left[\frac{1-q^{*2}}{1-\beta(1-q^{*2})}(1,0,\ldots,0,1,-2)\right.$$
$$\left.+(-2,0,\ldots,0,2)\right] + \mathcal{O}(1-\nu)^3.$$

It is not *a priori* clear that the proposed expansion in powers of $1-\nu$ will converge. However, numerical analysis shows this to be the case for some finite region in the $T < 2\nu - 1$ part of the $T/\nu$ phase diagram.

We may now conclude that, as far as fixed-points are concerned, there are effectively three regions in the $T/\nu$ phase diagram:

(i) Region $P$ ($T > 1$):

$q$ fixed-point $\Rightarrow q = 0$ (paramagnetic region)

(ii) Region $M$ ($2\nu - 1 < T < 1$):

$q$ fixed-point $\Rightarrow q = 0$ or $q = \pm q^+$ (full mixture region)

(iii) Region $H$ ($T < 2\nu - 1$):

Non-trivial types of fixed-points $q$ (Hopfield region).

An important feature is that for odd $p$ there must be a first-order transition in (or at the boundary of) region $H$, since we found that the only non-trivial fixed-points that can be obtained by repeated continuous bifurcations from the $T > 1$ fixed-point $q = 0$ are the full mixtures $q = \pm q^+$. Therefore the Hopfield-type fixed-points in region $H$ must appear as discontinuous bifurcations. Only for $p$ even is it possible that all fixed-points can be obtained from a scenario of repeated continuous bifurcations from $q = 0$. For $p = 2$ we have indeed found a second-order transition, however, for even $p > 2$ one finds, by solving the fixed-point equations numerically, that the bifurcations of Hopfield-type fixed-points in region $H$ are discontinuous and therefore the corresponding transition is first order (as for odd $p$). Furthermore, solving the fixed-point equations numerically shows that the location of the first-order transition line seems not to depend much on the dimension $p$, and is in good approximation given by

$$\nu_c(T) = \tfrac{1}{2} + T - T^2 + \tfrac{3}{4}T^3 - \tfrac{1}{4}T^4.$$

In section 6 we will present numerical evidence for this relation. The resulting picture of the system with respect to how the possible fixed-points are determined by the system parameters $T$ and $\nu$ is summarized in the phase diagram of figure 2.

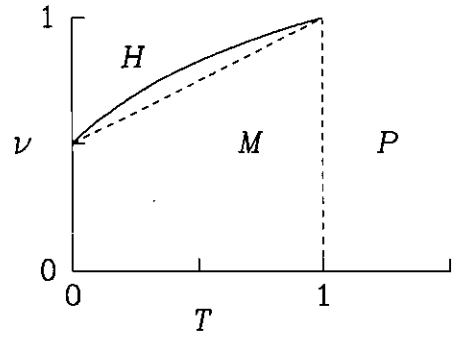


**Figure 2.** The types of fixed-points possible: $P$, paramagnetic region, $q = 0$; $M$, mixture region, $q = q(T)(1,\ldots,1) \neq 0$; $H$, Hopfield region, $\exists \mu\rho : q_\mu \neq q_\rho$. The full curve is the first-order transition and the vertical broken line is the second-order transition.

## 4. Stability of fixed-points

In this section we will analyse the stability properties of the fixed-points as calculated in the previous section for both parallel dynamics (Markov process) and sequential dynamics (master equation). In the case of parallel dynamics (9) the criterion for a fixed-point $q$ to be stable is

$$\lim_{|\delta q(t)|\to 0} \frac{|\delta q(t+1)|}{|\delta q(t)|} < 1.$$

According to the definition (9) this implies

$$\max_{x} \frac{x \cdot A^\dagger \Gamma^2(q) A x}{x^2} < T^2 \tag{25}$$

where $x$ is real valued and the matrix $\Gamma$ is defined in (17). In the case of sequential dynamics we have to study the behaviour of (8) around a fixed-point $q$, which is determined by the Hessian matrix. The criterion for a fixed-point $q$ to be stable is now given by

$$\max_{x} \frac{x \cdot \frac{1}{2}\left[\Gamma(q)A + A^\dagger \Gamma(q)\right] x}{x^2} < T. \tag{26}$$

### *4.1. Stability of the trivial fixed-point*

Let us first turn to the stability of the trivial fixed-point $q = 0$. Since $\Gamma(0) = 1$ (the identity matrix) we can conclude

$$\max_{x} \frac{x \cdot A^\dagger \Gamma^2(q) A x}{x^2} = \langle 0 | A^\dagger A | 0 \rangle = 1$$

$$\max_{x} \frac{1}{2} \frac{x \cdot \left[\Gamma(q)A + A^\dagger \Gamma(q)\right] x}{x^2} = \frac{1}{2}\langle 0 | \left[A + A^\dagger\right] | 0 \rangle = 1$$

(the complete orthogonal basis $\{|n\rangle\}$ being defined in (10)). Therefore for both types of dynamics one finds:

$$T > 1 : \quad q = 0 \text{ is stable} \qquad T < 1 : q = 0 \text{ is unstable.}$$

*4.2. Stability of the fully symmetric fixed-point: general properties*

The next fixed-point to be analysed is the fully symmetric mixture state $q^+$ (22). The matrix $\Gamma(q^+)$ has been calculated previously (24):

$$\Gamma(q^+) = D^+[\beta] + R^+[\beta]|0\rangle\langle 0|.$$

We can always write the real-valued ($p$-dimensional) vector $x$ in equations (25) and (26) in terms of the basis $\{|n\rangle\}$:

$$x = \sum_{n=0}^{p-1} x_n|n\rangle \qquad (\forall n:\ x_{p-n} = x_n^*)$$

where the proviso $x_{p-n} = x_n^*$ reflects the restriction that $x$ must be real-valued. The full mixture $q^+$ is certainly stable with regard to fluctuations in its amplitude (which follows from (22)). Therefore we can take $x_0 = 0$. The criteria for $q^+$ to be stable now become:

$$\text{Parallel dynamics:} \quad \max_{x,\forall n:\ x_{p-n}=x_n^*} \frac{\sum_{n=1}^{p-1}|x_n|^2|a_n|^2}{\sum_{n=1}^{p-1}|x_n|^2} < \frac{1}{\beta^2 D^+[\beta]^2} \tag{27}$$

$$\text{Sequential dynamics:} \quad \max_{x,\forall n:\ x_{p-n}=x_n^*} \frac{\sum_{n=1}^{p-1}|x_n|^2 \operatorname{Re} a_n}{\sum_{n=1}^{p-1}|x_n|^2} < \frac{1}{\beta D^+[\beta]}. \tag{28}$$

Here the quantities $a_n$ are the eigenvalues of the matrix $A$ (11):

$$a_n \equiv \nu + (1-\nu)e^{-2\pi i n/p}$$

Using the relations $|a_{p-n}| = |a_n|$ and $\operatorname{Re} a_{p-n} = \operatorname{Re} a_n$ we can conclude that the maxima in (27) and (28) are obtained by choosing $x_n = x\delta_{n,1} + x^*\delta_{n,p-1}$, which enables us to write the criteria for $q^+$ to be stable as follows.

$$\text{Parallel dynamics:} \quad \left\{\nu^2 + (1-\nu)^2 + 2\nu(1-\nu)\cos(2\pi/p)\right\}^{1/2} < 1/(\beta D^+[\beta]) \tag{29}$$

$$\text{Sequential dynamics:} \quad \nu + (1-\nu)\cos(2\pi/p) < 1/(\beta D^+[\beta]). \tag{30}$$

From these expressions several conclusions can be drawn already:

(i) If $q^+$ is stable under parallel dynamics it is also stable under sequential dynamics.

(ii) For $\nu = 1$ the stability properties of $q^+$ are the same for the two types of dynamics.

(iii) If $q^+$ is stable for $\nu = 1$ is is stable for all $0 \leqslant \nu \leqslant 1$ (for both types of dynamics).

(iv) In the case of parallel dynamics the stability region in the $T/\nu$ phase diagram of $q^+$ is symmetric under reflection in the line $\nu = \frac{1}{2}$ (i.e. invariant under $\nu \to 1-\nu$).

The stability properties near the lines $T = 0$ and $T = 1$ of $q^+$ can be calculated analytically, without having to resort to numerical analysis of the inequalities (29) and (30).

First we will consider $T = 0$. If $p$ is odd we know from the thermodynamic analysis of the Hopfield model [3] that for $\nu = 1$ the mixture state $q^+$ is stable.

Therefore we may conclude that $q^+$ must be stable at $T = 0$ for all $0 \leqslant \nu \leqslant 1$. For even $p$ and $\nu = 1$ the state $q^+$ is unstable at $T = 0$ [3], however, it might stabilize for $\nu < 1$. In the case where $p$ is even one can easily show that

$$\lim_{\beta\to\infty} D^+[\beta] = \frac{p}{p-1}2^{-p}\binom{p}{p/2} > 0.$$

Therefore $\beta D^+[\beta] \to \infty$ as $\beta \to \infty$. For parallel dynamics and $p$ even it now follows from (29) that at $T = 0$ the mixture $q^+$ is always unstable. For sequential dynamics it follows from (30) that $q^+$ is stable only if $p = 2$ and $\nu < \frac{1}{2}$.

We now turn to the stability of $q^+$ near the line $T = 1$. Expansion of the amplitude $q^+[\beta]$ in powers of $\beta - 1$ gives (22):

$$q^+[\beta] = \left[\frac{3p}{3p-2}\right]^{1/2}\sqrt{\beta-1} + \mathcal{O}(\beta-1)^{3/2}.$$

We can now expand $\beta D^+[\beta]$ near $T = 1$, with the result

$$\beta D^+[\beta] = 1 + (\beta-1)\left[\frac{p+2}{p-1} - \frac{3p^2}{3p-2}\right] + \mathcal{O}(\beta-1)^2.$$

This expansion shows that for $p > 2$: $\mathrm{d}\{\beta D^+[\beta]\}/\mathrm{d}\beta|_{\beta=1} < 0$. This, in turn, implies that near $T = 1$ the inequalities (29) and (30) will hold (since the left-hand side of both inequalities is always below 1). Clearly for all $p > 2$ the full mixture state $q^+$ is stable near $T = 1$.

Having investigated the stability properties of $q^+$ at the boundaries $T = 0$ and $T = 1$ we will now study the limits $p$ small (i.e. $p$=2) and $p \to \infty$. The simplest case, for which determining the regions of stability becomes trivial, is to consider $p = 2$. In this case $D^+[\beta] = 1$ and from (29) and (30) one can immediately deduce:

$q^+$ stable (parallel dynamics): $T > |2\nu - 1|$

$q^+$ stable (sequential dynamics): $T > 2\nu - 1$.

In order to find the large $p$ behaviour of the amplitude $q^+[\beta]$ we will have to work out the pattern averages in (22) and in the definition of $D^+[\beta]$ for large $p$ and $1 < \beta < \infty$:

$$q^+ = \int \mathrm{d}z\, P(z) z \tanh(\beta q^+ z) \tag{31}$$

$$\beta D^+[\beta] = \frac{\beta p}{p-1}\int \mathrm{d}z\, P(z)\left[1 - \frac{z^2}{p}\right]\left[1 - \tanh^2(\beta q^+ z)\right] \tag{32}$$

where

$$P(z) \equiv \left\langle \delta\left[z - \frac{1}{\sqrt{p}}\sum_{\mu=1}^{p}\xi_\mu\right]\right\rangle_{\xi} = \int \frac{\mathrm{d}k}{2\pi} \mathrm{e}^{\mathrm{i}kz + p\log\cos(k/\sqrt{p})}$$

$$= \left[1 - \frac{1}{12p}(z^4 - 6z^2 + 3)\right]\frac{1}{\sqrt{2\pi}}\mathrm{e}^{-z^2/2} + \mathcal{O}(p^{-2}).$$

In order to facilitate the expansion of (31) and (32) we will define:

$$q^+[\beta] \equiv q_0 + q_1(1/p) + \mathcal{O}(p^{-2})$$

$$L_n \equiv \beta \int \frac{\mathrm{d}z}{\sqrt{2\pi}} z^n \mathrm{e}^{-z^2/2} \left[1 - \tanh^2(\beta q_0 z)\right]$$

Expanding (31) and comparing the first two orders gives (since $\beta > 1$):

$$L_0 = 1 \qquad q_1[1 - L_2] = \tfrac{1}{12} q_0[1 + 2L_2 - L_4].$$

Expansion of (32) in turn gives:

$$\beta D^+[\beta] = L_0 + \frac{1}{p}\left[\frac{3}{4}L_0 - \frac{1}{2}L_2 - \frac{1}{12}L_4 - \frac{q_1}{q_0}[L_0 - L_2]\right] + \mathcal{O}(p^{-2})$$

$$= 1 + \frac{2}{3p}[1 - L_2] + \mathcal{O}(p^{-2}).$$

Note that

$$L_2 = L_0 - 2\beta^2 q_0 \int \frac{\mathrm{d}z}{\sqrt{2\pi}} \mathrm{e}^{-z^2/2} z \tanh(\beta q_0 z)\left[1 - \tanh^2(\beta q_0 z)\right] < L_0 = 1.$$

We may now conclude from (29) and (30) that for all $\beta > 1$ and for all $\nu$ the mixture state $q^+$ will eventually become unstable as $p \to \infty$, since

$$\frac{1}{\beta D^+[\beta]} - \left\{\nu^2 + (1-\nu)^2 + 2\nu(1-\nu)\cos(2\pi/p)\right\}^{1/2}$$

$$= -\frac{2}{3p}[1 - L_2] + \mathcal{O}(p^{-2})$$

$$\frac{1}{\beta D^+[\beta]} - \nu - (1-\nu)\cos(2\pi/p) = -\frac{2}{3p}[1 - L_2] + \mathcal{O}(p^{-2}).$$

Apparently the width of the regions of stability near $T = 1$ and (if $p$ is odd) near $T = 0$ vanishes as $p \to \infty$.

We can now summarize the stability properties of $q^+$ ($\beta > 1$) for the limiting cases considered:

(i) $p = 2$:

parallel dynamics: $q^+$ is stable $\Leftrightarrow$ $T > |2\nu - 1|$

sequential dynamics: $q^+$ is stable $\Leftrightarrow$ $T > 2\nu - 1$.

(ii) $p \to \infty$: $q^+$ is unstable for all $0 < T < 1$

(iii) $T = 0$ ($p > 2$):

$p$ even: $q^+$ is unstable

$p$ odd: $q^+$ is stable

(iv) $T \to 1$: $q^+$ is stable for all $p > 2$.

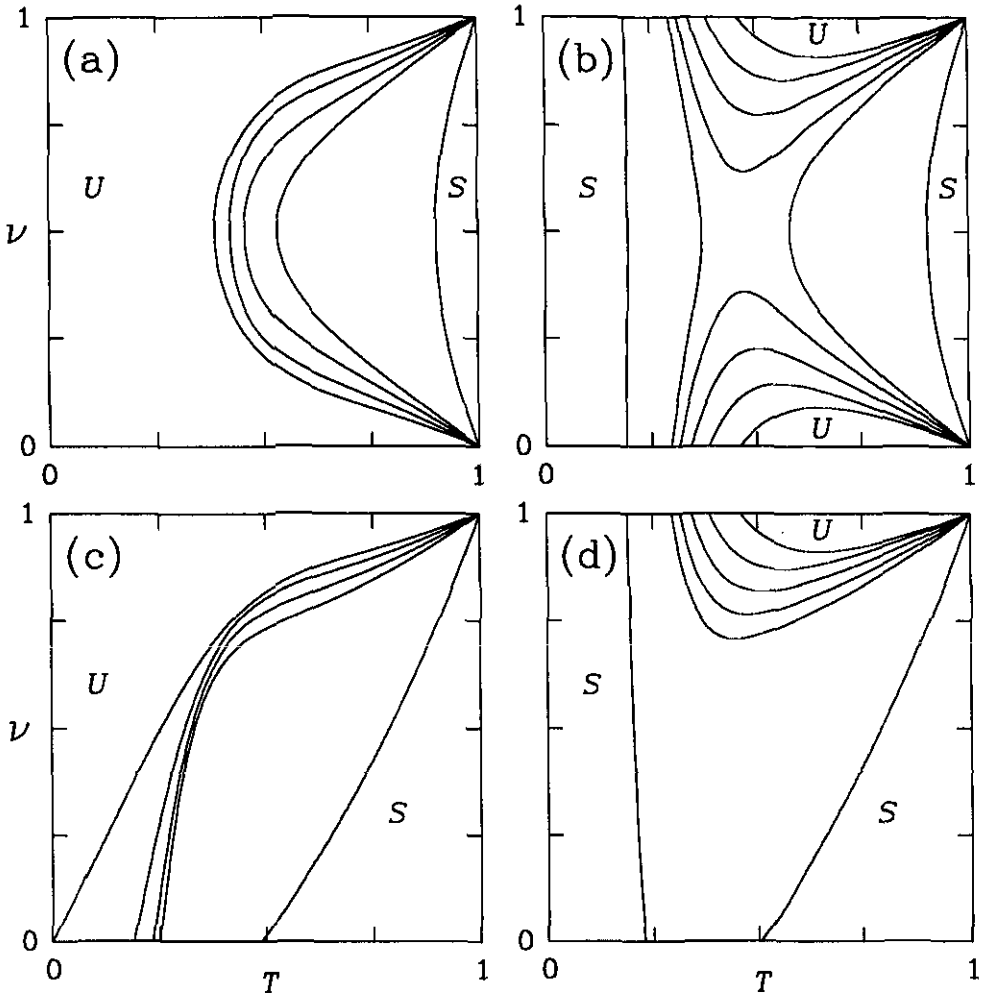


**Figure 3.** Stability boundaries of the full mixture fixed-point $q^+$ ($U$, unstable; $S$, stable): (*a*) parallel dynamics, $p \in \{4,6,8,10,40\}$ (going from $U$ to $S$); (*b*) parallel dynamics, $p \in \{3,5,7,9,11,41\}$ (going from $U$ to $S$); (*c*) sequential dynamics, $p \in \{4,6,8,10,40\}$ (going from $U$ to $S$); and (*d*) sequential dynamics, $p \in \{3,5,7,9,11,41\}$ (going from $U$ to $S$).

### *4.3. Stability of the fully symmetric fixed-point: the full phase diagram*

Having analysed the stability of $q^+$ for both $p = 2$ and $p \to \infty$ as well as in the limits $T \to 0$ and $T \to 1$ we will now study, by solving the relevant equations (29) and (30) numerically, the stability properties for arbitrary values of $T$, $\nu$ and $p$. The case $p = 2$ being analysed in full in a previous section, we here focus on $p > 2$. Figure 3 shows the regions of stability for the fully symmetric mixture state $q^+$ for parallel dynamics with $p$ even (*a*) or odd (*b*), as well as for sequential dynamics with $p$ even (*c*) or odd (*d*).

First we consider parallel dynamics. For $p$ even (*a*) there is simply one boundary line, separating the stability region (near $T = 1$) from the region of instability (near $T = 0$). For $p$ odd (*b*) there are two boundary lines: for small $p$ in most of the phase

diagram the state $q^+$ is stable (the exceptions consisting of two small unstable regions near $\nu = 0$ and $\nu = 1$). If $p$ (odd) increases, the two regions of instability grow and finally merge. For large $p$ (odd) there are two boundary lines, separating two regions of stability (near $T = 0$ and near $T = 1$, respectively) from a region of instability (near $T = \frac{1}{2}$). Clearly the main difference between $p$ even and $p$ odd is that in the latter case there are two separate regions of stability. Apart from this difference, for large $p$ the results for $p$ even and $p$ odd are similar in the sense that in both cases the fixed-point $q^+$ will eventually become unstable for all $(T, \nu)$ as $p \to \infty$.

Next we consider sequential dynamics. For $p$ even (*c*) there is again one boundary line, separating the stability region (near $T = 1$) from the region of instability (near $T = 0$). For small odd $p$ (*d*) in most of the phase diagram the state $q^+$ is stable (the exception being a small unstable region near $\nu = 1$). If $p$ (odd) increases this region of instability grows. For large $p$ (odd) there are two boundary lines, separating two regions of stability (near $T = 0$ and near $T = 1$, respectively) from a region of instability (near $T = \frac{1}{2}$). Again the main difference between $p$ even and $p$ odd is that in the latter case there are two separate regions of stability (if $p$ is sufficiently large). Apart from this difference, for large $p$ the results for $p$ even and $p$ odd are again similar in the sense that in both cases the fixed-point $q^+$ will eventually become unstable for all $(T, \nu)$ as $p \to \infty$. These results confirm the limiting properties derived analytically in the previous section.

If we compare the outcome of the two types of dynamics we observe that in the case of parallel dynamics all stability regions are symmetric with respect to reflection in the line $\nu = \frac{1}{2}$ (in contrast to the stability regions for sequential dynamics). As will be shown in the next section, this symmetry in the phase diagram can be understood as being the result of symmetries of the underlying dynamics. A further surprising result is that for $p \to \infty$, even in the case of sequential dynamics, in all of the region $2\nu - 1 < T < 1$ the system will evolve towards a non-stationary solution of the dynamic equations (since all fixed-points are found to be unstable). Most studies published so far, in which the reproduction of sequences of random unbiased patterns with sequential dynamics is studied, conclude that without additional stabilizing mechanisms (or a complicated matrix as in [22]) the $\nu = 0$ system will evolve towards the fully symmetric mixture state. However, these conclusions are based on simulation studies with rather moderate values for $p$, whereas the stability of non-stationary solutions (according to figure 3) requires $p$ to be sufficiently large.

It must be emphasized that stability of the fixed-point $q^+$ does not automatically imply a large basin of attraction. For instance, numerical iteration of (9) shows that, although for odd $p$ the fixed-point $q^+$ is stable near $T = 0$, in this region of the phase diagram the unstable pure states $q_\mu = \delta_{\mu\rho}$ are in the domain of attraction of limit-cycle attractors. If one, finally, studies the stability properties (for $p$ even and $T > 2\nu - 1$) of the alternating mixture $q^-$, one finds this fixed-point to be unstable for all $T,\nu$.

## 5. Symmetries

In this section we will exploit the symmetries in the distribution $\rho$ of the vectors $\xi$ and establish relations between the solutions of the nonlinear dynamical laws. Apart from two trivial operations (index shift $S$ and reflection in the origin) we show that, for parallel dynamics, there is a duality that relates all trajectories in the upper part of

the phase diagram ($\nu > \frac{1}{2}$) to the trajectories in the lower part of the phase diagram ($\nu < \frac{1}{2}$).

*5.1. Symmetry mappings*

The set $\mathcal{G}$ is defined as the set of all linear transformations $G$ under which the probability distribution $\rho(\xi)$ is invariant:

$$G \in \mathcal{G} : \rho(G\xi) = \rho(\xi) \qquad \forall \xi \in \{-1,1\}^p.$$

It consists of all combinations of reflections in the elementary planes $\xi_\lambda = 0$ and axis permutations. Each element $G$ in $\mathcal{G}$ is a matrix of the form:

$$G_{\mu\rho} = c_\mu \delta_{\mu,\pi(\rho)} \qquad c_\mu \in \{-1,1\}$$

$$\pi : \{1,\ldots,p\} \to \{1,\ldots,p\} \qquad \text{(invertible)}.$$

If $G \in \mathcal{G}$ one can deduce that

$$G\langle \xi \tanh[\beta\xi \cdot Aq]\rangle_\xi = \langle \xi \tanh[\beta\xi \cdot GAq]\rangle_\xi.$$

We can now define symmetry mappings in the following way: $G \in \mathcal{G}$ is a symmetry mapping if and only if

$$\exists G' \in \mathcal{G} \text{ such that } \forall \nu \in [0,1] : GA_\nu = A_{\gamma(\nu)}G' \text{ for some } \gamma(\nu) \in [0,1].$$

In this section the matrix $A$ will carry as an index the value of the parameter $\nu$, used in its definition (2). The reason is that we will be considering relations between successive state vectors in systems which are different with respect to this parameter. The above definition selects from the set $\mathcal{G}$ those mappings that enable us to relate the right-hand side of (33) in turn to the evolution in time of some state vector $G'q$. Using the general form of the matrices $G \in \mathcal{G}$ one can show that the problem of finding all symmetry mappings (i.e. all $G \in \mathcal{G}$ such that (34) holds) has two types of solution only:

$$\gamma = \nu : \qquad [G,S] = 0 \qquad G' = G$$

$$\gamma = 1-\nu : \qquad SG = GS^\dagger \qquad G' = GS$$

with the permutation matrix $S$, defined in (2). Again we can use the general form of the matrices $G \in \mathcal{G}$ to calculate these two types of solution explicitly:

$$\gamma = \nu : \qquad G = G' = \pm S^n \qquad (n = 0, \pm 1, \pm 2, \ldots) \tag{35}$$

$$\gamma = 1-\nu : \qquad G = \pm KS^n \qquad G' = GS \qquad (n = 0, \pm 1, \pm 2, \ldots) \tag{36}$$

where

$$K_{\lambda,\rho} \equiv \delta_{\lambda,p+1-\rho}(\bmod p).$$

Some of the properties of the matrix $K$ in relation to $S$, $S^\dagger$ and the basis $\{|n\rangle\}$ are given in section 2.

The set of symmetry mappings (35) with $\gamma = \nu$ is generated by the two operations $\{-1, S\}$ (note: $S^{\dagger n} = S^{p-n}$). They imply the following

(i) If the vectors $\{q_0, q_1, q_2, \ldots\}$ correspond to a solution of the parallel dynamics (9) for a certain value of the parameter $\nu$, then the same is true for $\{-q_0, -q_1, -q_2, \ldots\}$ and $\{Sq_0, Sq_1, Sq_2, \ldots\}$.

(ii) If the trajectory $q(t)$ corresponds to a solution of the sequential dynamics (8) for a certain value of the parameter $\nu$, then the same is true for $-q(t)$ and $Sq(t)$.

These relations reflect more or less trivial symmetries of the problem.

The second (non-trivial) set of symmetry operations (36) with $\gamma = 1 - \nu$ is, apart from the two operations $\{-1, S\}$ we have already discussed, generated by the matrix $K$. In the case of sequential dynamics relation (36) cannot be used for establishing relations between different solutions of the problem (8). In the case of parallel dynamics, however, we can deduce from (36) the statement

(iii) If the vectors $\{q_0, q_1, q_2, \ldots\}$ correspond to a solution of the parallel dynamics (9) for a certain value of the parameter $\nu$, then a solution of the parallel dynamics for the value $1 - \nu$ is given by $\{Kq_0, SKq_1, S^2Kq_2, \ldots, S^nKq_n, \ldots\}$.

Apparently for parallel dynamics there is a well-defined correspondence between the solutions of the evolution equations for the order parameters $q$ in the upper part of the $T/\nu$ phase diagram and the solutions in the lower part of this phase diagram. This might have been guessed from the symmetry of the stability diagram of the full mixture fixed-point $q^+$.

### *5.2. Parallel dynamics: the $\nu/1-\nu$ duality*

We will now show that for parallel dynamics there is actually a 1–1 correspondence between all solutions of (9) in the upper half of the $T/\nu$ phase diagram ($\nu > \frac{1}{2}$) and all solutions in the lower half of the phase diagram ($\nu < \frac{1}{2}$). We will first define the set $\mathcal{L}_\nu$ of solutions for a given value of the parameter $\nu$. Consider an infinite sequence $Q$ of $p$-dimensional real-valued vectors:

$$Q = \{q_0, q_1, q_2, \ldots\}.$$

The set of all such sequences will be called $\mathcal{L}$. The set $\mathcal{L}_\nu \subset \mathcal{L}$ will now simply be the set of all sequences $Q \in \mathcal{L}$, such that the constituent vectors $q_n$ correspond to successive iterations of the parallel dynamics (37) for the parameter value $\nu$:

$$\mathcal{L}_\nu \equiv \{\, Q \in \mathcal{L} \mid \forall n \geqslant 0 :\ q_{n+1} = \langle \xi \tanh[\beta \xi \cdot A_\nu q_n] \rangle_\xi \,\}. \tag{37}$$

Clearly each sequence $Q \in \mathcal{L}_\nu$ is completely defined by its first state vector $q_0$. In terms of the sets (37) we can write the correspondence relation resulting from (36) as

$$Q \in \mathcal{L}_\nu \ \Rightarrow\ \mathcal{D}Q \in \mathcal{L}_{1-\nu}$$

where the linear operation $\mathcal{D}$ is defined as

$$\mathcal{D} :\ \mathcal{L} \to \mathcal{L}$$

$$\forall n \geqslant 0 : \qquad [\mathcal{D}Q]_n \equiv D_n q_n \qquad D_n \equiv S^n K \tag{38}$$

Since the matrices $D_n$ are Hermitian and unitary it immediately follows from the definition (38) that:

$$\mathcal{D}^2 = 1$$

which implies that for each value of $\nu$ there is a 1–1 correspondence between all elements in $\mathcal{L}_\nu$ and all elements in $\mathcal{L}_{1-\nu}$ (a duality between the sets $\mathcal{L}_\nu$ and $\mathcal{L}_{1-\nu}$):

$$Q \in \mathcal{L}_\nu \Leftrightarrow \mathcal{D}Q \in \mathcal{L}_{1-\nu} \qquad \mathcal{D}(\mathcal{D}Q) = Q. \tag{39}$$

It is clear that the stability properties of $Q = \{q_0, q_1, q_2, \ldots\} \in \mathcal{L}_\nu$ and $\mathcal{D}Q = \{q_0' q_1', q_2', \ldots\} \in \mathcal{L}_{1-\nu}$ must be the same, since $|\delta q_n'| = |D_n \delta q_n| = |\delta q_n|$.

A sequence $Q = \{q_0, q_1, q_2, \ldots\} \in \mathcal{L}$ will be called $l$-periodic if $\forall n \geqslant 0 : q_{n+l} = q_n$. A sequence $Q = \{q_0, q_1, q_2, \ldots\} \in \mathcal{L}$ corresponds to a fixed-point of the dynamics (9) if $\forall n > 0 : q_n = q_0$. We will now simply list a few of the properties of the duality $\mathcal{D}$ which can be easily verified:

$$Q = \{q_0, q_1, q_2, \ldots\} \qquad \mathcal{D}Q = \{q_0', q_1', q_2', \ldots\}$$

(i) $\forall n \geqslant 0 : |q_n'| = |q_n|$;
(ii) $\forall n \geqslant 0 : \langle 0|q_n'\rangle = \langle 0|q_n\rangle$;
(iii) $\forall n \geqslant 0 : \langle p/2|q_n'\rangle = (-1)^{n+1}\langle p/2|q_n\rangle$;
(iv) $Q$ is $l$-periodic $\Rightarrow \mathcal{D}Q$ is $lp$-periodic;
(v) $Q$ is $lp$-periodic $\Leftrightarrow \mathcal{D}Q$ is $lp$-periodic;
(vi) $Q$ represents a fixed point $\Rightarrow \mathcal{D}Q$ is $p$-periodic;
(vii) $\mathcal{D}\{q^+, q^+, \ldots\} = \{q^+, q^+, \ldots\}$.

Clearly this duality, resulting from symmetry properties of the dynamics (9) explains why the stability diagram of the full mixture state $q^+$ is symmetric with respect to the interchange $\nu \to 1 - \nu$. It also indicates that with each stable non-symmetric fixed-point in the Hopfield region $T < 2\nu - 1$ will correspond a stable $p$-periodic limit cycle in the region $T < 1 - 2\nu$. This, in turn, implies that to the first-order transition line $\nu_+(T)$ in the region $T < 2\nu - 1$ (between stable Hopfield-type fixed-points and either the full mixture state $q^+$ or a limit-cycle attractor) there must correspond a first-order transition line $\nu_-(T)$ in the region $T < 1 - 2\nu$, which separates the low-temperature region where there are stable $p$-periodic limit cycles (different from the fixed-point $q^+$) from the region where such limit cycles do not exist.

If we finally choose the initial state $q_0$ of the sequence $Q$ to be a pure state (i.e. $q_0 = q_0 \hat{e}_\rho$ for some $\rho$), we can use the relation $Kq_0 = S^{1-2\rho}q_0$ and the fact that $S$ is a symmetry mapping to derive:

$$Q \equiv \{q_0\hat{e}_\rho, q_1, \ldots, q_n, \ldots\} \qquad Q' \equiv \{q_0\hat{e}_\rho, S^{2\rho}Kq_1, \ldots, S^{n+2\rho-1}Kq_n, \ldots\}$$
$$Q \in \mathcal{L}_\nu \Leftrightarrow Q' \in \mathcal{L}_{1-\nu}.$$

Once we know which is the trajectory followed by the state vector upon choosing a pure initial state $q_0\hat{e}_\rho$ in the upper part of the $T/\nu$ phase diagram, we can immediately construct the trajectory that starts in the very same initial pure state $q_0\hat{e}_\rho$ for the lower part of the phase diagram. Furthermore both amplitude and $|0\rangle$ component of the two evolving state vectors will always be the same, since

$$|S^{n+2\rho-1}K\boldsymbol{x}| = |\boldsymbol{x}| \qquad \langle 0|[S^{n+2\rho-1}K]\boldsymbol{x}\rangle = \langle 0|\boldsymbol{x}\rangle.$$

If the initial pure state $q_0\hat{e}_\rho$ is in the attraction domain of some non-trivial fixed-point $q^*$ we obtain

$$q_0^{(\nu)} = q_0^{(1-\nu)} \equiv q_0\hat{e}_\rho :$$
$$\lim_{n\to\infty} q_n^{(\nu)} = q^* \Rightarrow q_n^{(1-\nu)} \to S^{n+2\rho-1}Kq^* \qquad (n \to \infty)$$
$$\left[S^{n+2\rho-1}Kq^*\right]_\mu = q^*_{n-\mu+2\rho}.$$

If $q^* = q^+$, i.e. the pure state $q_0\hat{e}_\rho$ is in the domain of attraction of the full mixture state for parameter value $\nu$, then also for parameter value $1-\nu$ this pure state will flow towards $q^+$ (since $Kq^+ = Sq^+ = q^+$). If $q^* \neq q^+$ is a non-trivial fixed-point (in the region $T < 2\nu - 1$) we can immediately calculate the (stable) limit cycle to which $q_0\hat{e}_\rho$ will be driven for the parameter value $1-\nu$. The $1-\nu$ limit cycle $q'_n \equiv S^{n+2\rho-1}Kq^*$ represents a smooth periodic trajectory with period $p$, the state vectors of which can be calculated using the series expansion introduced for calculating the fixed-points $q^*$ in section 3.4.

## 6. Numerical iteration of the macroscopic laws

### *6.1. Periodic attractors*

In this section we will analyse some properties of the periodic solutions (note that for $p \to \infty$ in most of the phase diagram, $T > 2\nu - 1$, there will be no stable fixed-points). Since it is impossible to systematically vary both the model parameters $\nu$, $T$ and $p$ and all possible initial conditions $q_0$ in a numerical study of the system equations (8) and (9), we will restrict ourselves and present some typical examples of the behaviour observed. If, as a first step, one is only interested in the existence and amplitude of periodic attractors, it might be convenient to reduce the number of order parameters considered from $p$ to 2, by introducing the decomposition:

$$q(t) \equiv Q_s(t)(1,\ldots,1) + Q_d(t)\hat{q}^\perp(t)$$

$$Q_s(t) \equiv \frac{1}{p}\sum_\mu q_\mu(t) \qquad (1,\ldots,1)\cdot\hat{q}^\perp(t) = 0 \qquad Q_d \equiv |q(t) - Q_s(t)(1,\ldots,1)|.$$

For $T > 2\nu - 1$ the only possible fixed-point is $q^+$. In this region of the phase diagram the existence of a non-stationary solution is therefore equivalent to finding $Q_d > 0$.

We will first restrict ourselves to parallel dynamics (the behaviour of equation (9)). Figure 4 shows for $p = 9$, $T = 0.5$ and $\nu \in \{0.25, 0.5, 0.75\}$ the evolution in time of the overlaps $\{q_\mu\}$ (upper row) from a pure initial state $q_\mu = \delta_{\mu 1}$, as well as the evolution in time of the amplitudes $Q_s$ and $Q_d$ following 50 random draws of initial state vectors $q_0$ (lower row). Since, in terms of stability, we have previously found that the cases $p$ odd and $p$ even may be quite different, the results of similar experiments performed with $p = 10$ are shown in figure 5. From these figures we can draw some conclusions, which numerical experiments (performed for larger values of $p$ and different choice for $T$ and $\nu$) show to be quite generally valid:

(i) Starting from a pure initial state the system evolves towards a limit cycle, which depends on the parameter $\nu$ only through the value of its period $\Omega$.

(ii) The region in the phase diagram where pure states are in the domain of attraction of the full mixture $q^+$ is only a subset of the region where the full mixture is stable.

(iii) The amplitudes $|Q_s(t)|$ and $Q_d(t)$ tend towards stationary values for $t \to \infty$ (which do not dependent on the initial state).

The above conclusions seem to hold in general as long as $T > 2\nu - 1$ and $T > 1 - 2\nu$. If $T < 2\nu - 1$ or $T < 1 - 2\nu$ the amplitudes $|Q_s|$ and $Q_d$ will no longer be uniquely defined as soon as one passes the first-order transition lines

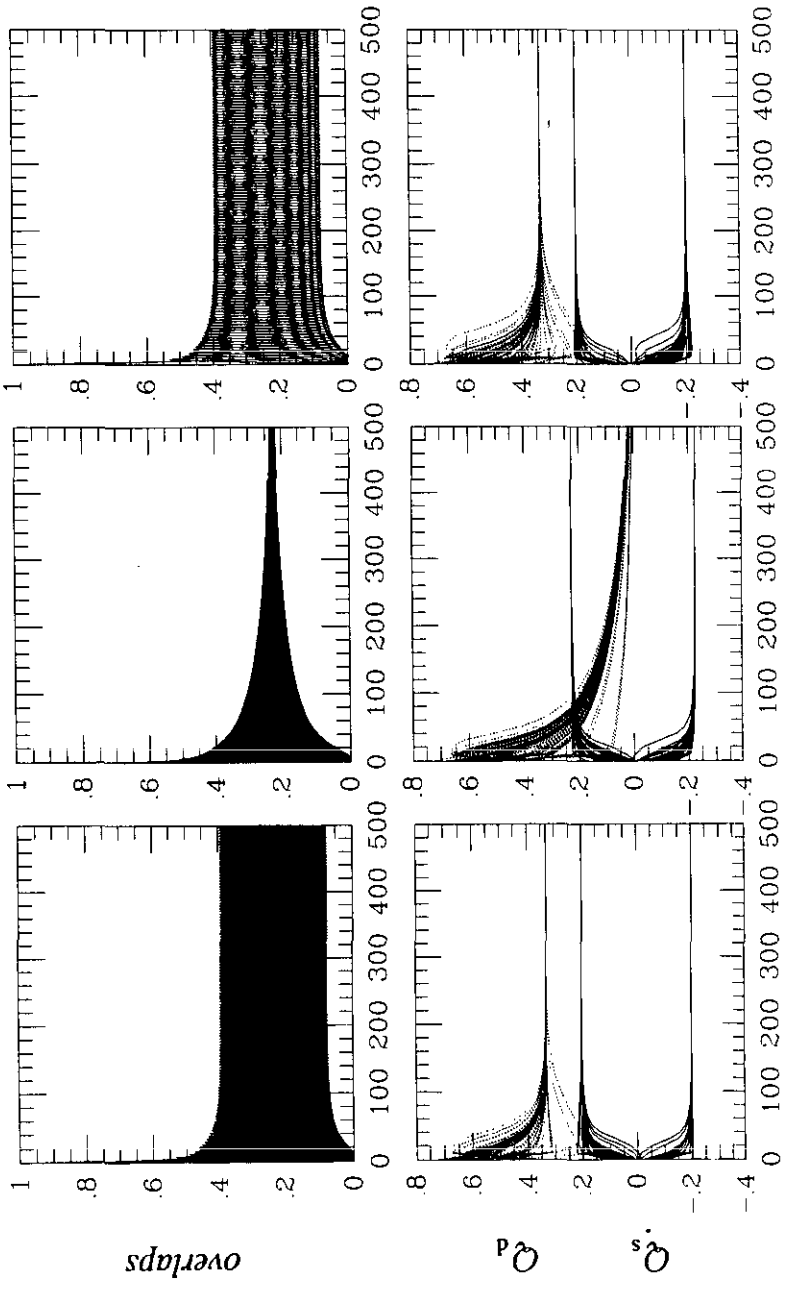


**Figure 4.** Numerical iteration of the macroscopic laws for $p = 9$ and $T = 0.5$ (parallel dynamics): upper row, evolution of $\{q_\mu\}$ $(\mu = 1 \ldots 9)$, starting from a pure state; lower row, evolution of $Q_s$ (full curves) and $Q_d$ (broken curves) following 50 randomly drawn initial state vectors $q_0$.

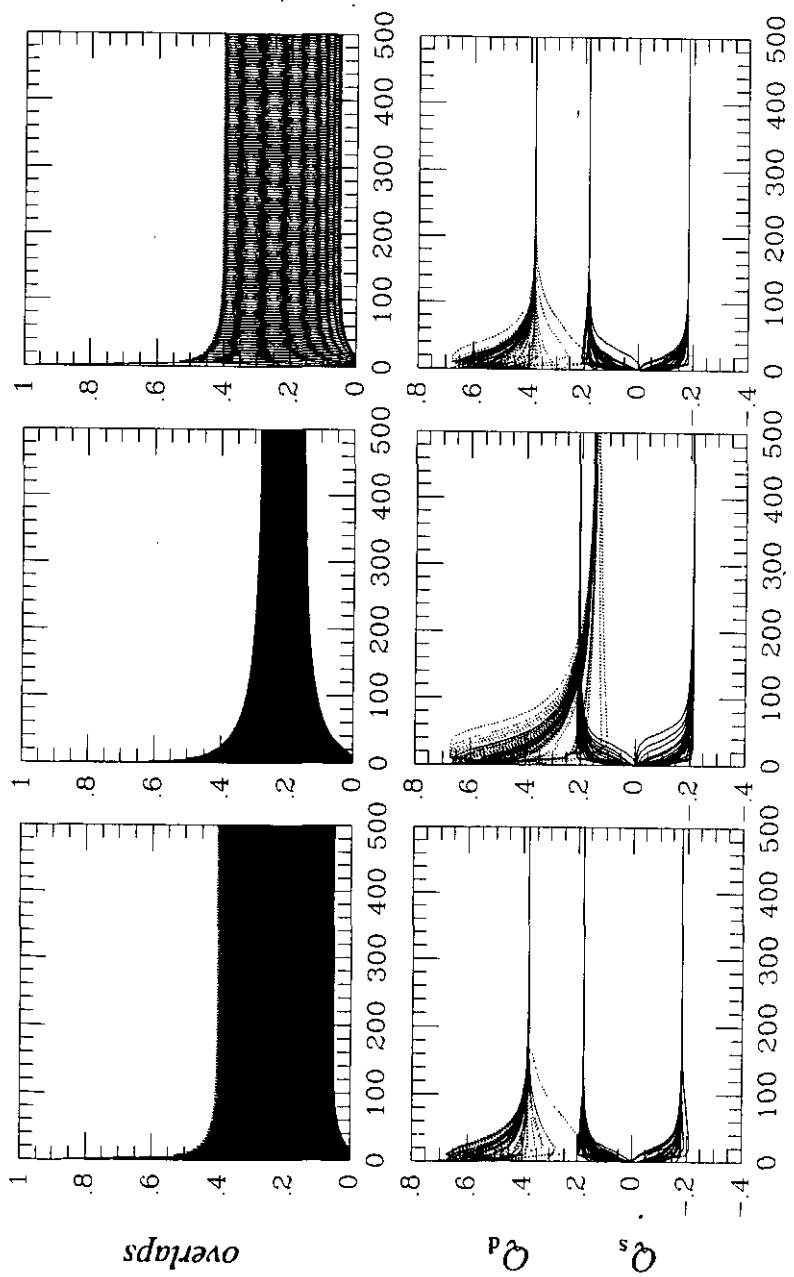


**Figure 5.** Numerical iteration of the macroscopic laws for $p = 10$ and $T = 0.5$ (parallel dynamics): upper row, evolution of $\{q_\mu\}$ $(\mu = 1 \ldots 10)$, starting from a pure state; lower row, evolution of $Q_s$ (full curves) and $Q_d$ (broken curves) following 50 randomly drawn initial state vectors $q_0$.

$\nu_{\pm}(T)$, which is due to the appearance of Hopfield-type fixed-points and their dual $p$-periodic limit cycles, respectively.

The huge amount of computer time involved prevented us from performing similar numerical studies for the case of sequential dynamics. The only feature we wish to illustrate is the somewhat surprising conclusion obtained from studying fixed-points and their stability: the fact that sequential dynamics allows for (non-fixed-point) periodic attractors. Figure 6 shows the result of iterating the macroscopic laws (8) for $p = 10$, $T = 0.1$ and $\nu = 0$, following a pure initial state. Data are shown (and connected) in $\Delta t = 1$ time intervals. Although systems with sequential dynamics indeed turn out to be able to exhibit oscillatory overlap evolutions (without having to introduce stabilizing mechanisms), the amplitude of these limit cycles is significantly smaller than the amplitude corresponding to parallel dynamics (at least for random patterns).

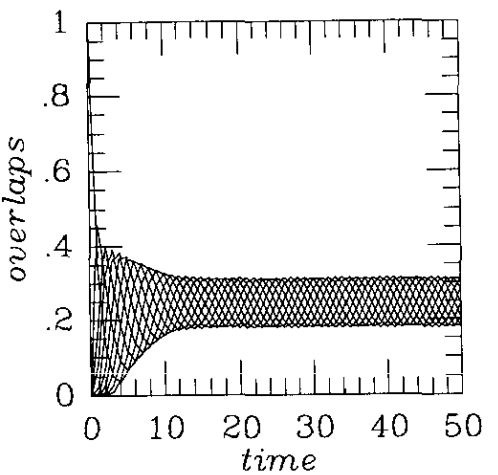


**Figure 6.** Numerical iteration of the macroscopic laws for sequential dynamics, starting from a pure state ($p = 10$, $T = 0.1$ and $\nu = 0$).

### 6.2. *The first-order transitions*

The property of the amplitudes $Q_d$ and $|Q_s|$ that in most of the phase diagram they evolve towards some ergodic value, enables us illustrate the first-order transitions in terms of these amplitudes. To fix their values uniquely in the regions $T < 2\nu - 1$ and $T < 1 - 2\nu$ as well, we consider only the (parallel) evolution in time following an intitial pure state $q_\mu(0) \equiv \delta_{\mu 1}$.

The equilibrium values found turn out to depend only on $|\nu - \frac{1}{2}|$ (as predicted by the $\nu/1 - \nu$ duality). Figure 7 shows as a function of temperature the equilibrium amplitudes $Q_d$ (upper row) and $Q_s$ (lower row) for $p = 9$ and $p = 10$ and $|\nu - \frac{1}{2}| \in \{0, 0.1, 0.2, 0.3, 0.4, 0.5\}$. Again, making different choices for the system parameters produces graphs which are only quantitatively different from the ones presented in figure 7. The first-order transitions at $\nu_{\pm}(T)$ are reflected in discontinuities in the amplitudes $Q_d$ and $Q_s$ as soon as $\nu < 1$. Only for $\nu = 1$ (the Hopfield model) and $p = 2$ (symmetric interaction matrix) are the transitions second order.

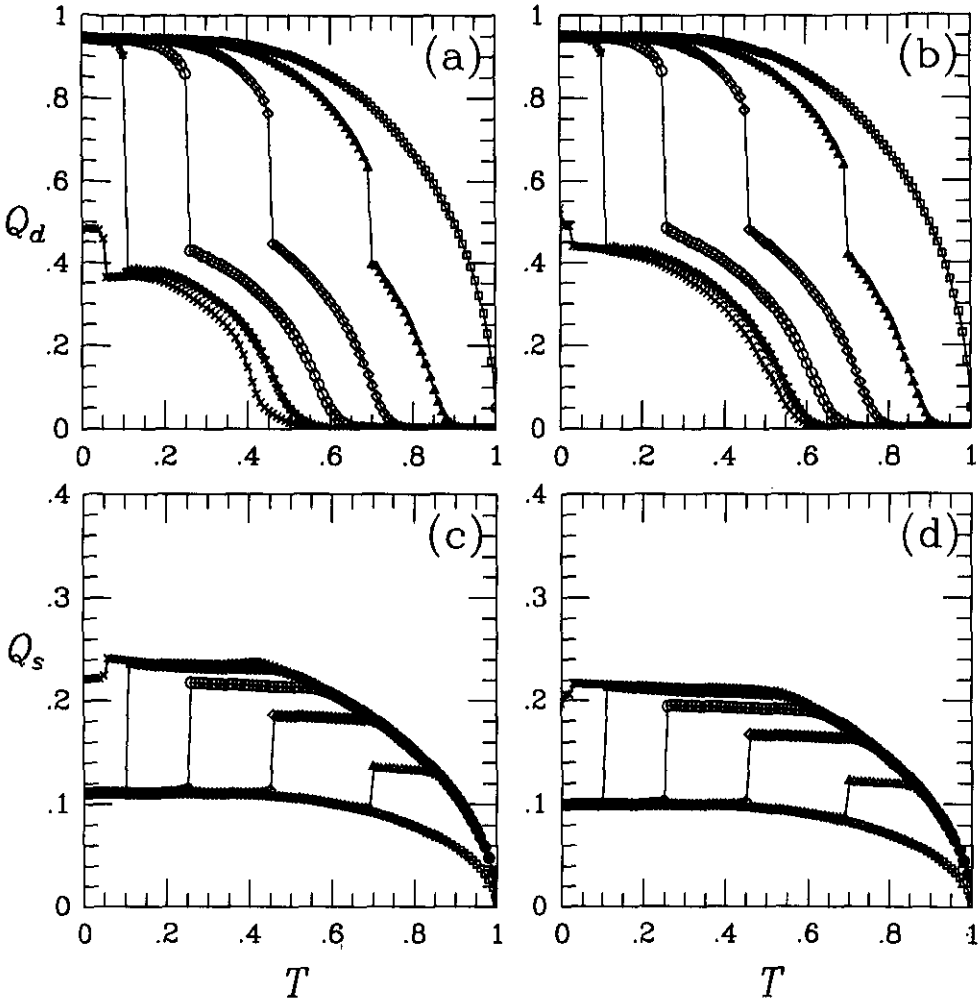


**Figure 7.** Equilibrium amplitudes as a function of temperature (parallel dynamics, numerically iterated following a pure initial state): $p = 9$, $Q_d$ (*a*) and $Q_s$ (*c*); $p = 10$, $Q_d$ (*b*) and $Q_s$ (*d*); □, $\nu \in \{0, 1\}$; △, $\nu \in \{0.1, 0.9\}$; ◇, $\nu \in \{0.2, 0.8\}$; ○, $\nu \in \{0.3, 0.7\}$; ⋆, $\nu \in \{0.4, 0.6\}$; ×, $\nu = 0.5$.

The locations in the phase diagram of the two first-order transition lines $\nu_{\pm}(T)$ are found not to depend much on the dimension $p$, as long as $p > 2$ (in contrast to the magnitude of the jumps at the discontinuities). It turns out that in good approximation the critical lines are given by

$$\nu_{\pm}(T) = \tfrac{1}{2} \pm T[1 - T + \tfrac{3}{4}T^2 - \tfrac{1}{4}T^3] \tag{40}$$

which are depicted in figure 8, together with the results of locating the first-order transition by numerical iteration of the parallel dynamical equations for $p \in \{3, 4, 9, 10\}$. The accuracy of the numerical data is $\Delta(T, \nu) = (0.002, 0)$; within this error margin there was no difference between the $p = 9$ and the $p = 10$ results. The corresponding data for sequential dynamics differ only in the absence of the $\nu < \frac{1}{2}$ transition line $\nu_{-}(T)$.

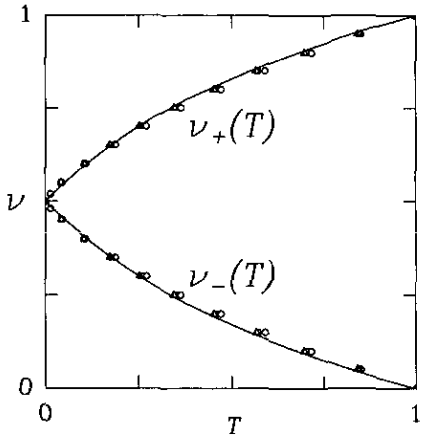


**Figure 8.** The first-order transition lines $\nu_\pm(T)$, together with corresponding numerical data: ○, $p = 3$; □, $p = 4$; △, $p = 9, 10$.

### *6.3. The attractor period $\Omega$ for parallel dynamics*

Finally we will study, for parallel dynamics, the dependence of the period $\Omega$ of the periodic attractors on the system parameters. For $\nu = 1$ (the Hopfield model) we know that the system will always settle into an equilibrium state. Using the duality of section 5.2 it now immediately follows that for $\nu = 0$ the system will evolve towards a stable period-$p$ limit cycle, i.e. $\Omega = p$ for $\nu = 0$. In order to find the period for intermediate values of $\nu$ we will make an ansatz for the solution of the dynamic equations (9), which is inspired by the numerical results of the previous sections:

$$q_\mu(t) \equiv f\left[\frac{\mu - \omega t + \phi}{p}\right] \qquad f[x+1] = f[x] \qquad (\forall x) \tag{41}$$

which simply amounts to assuming (quasi-) periodic trajectories with constant velocity (symmetric in the pattern indices). The period $\Omega$ can be written as $\Omega = p/\omega$. If we now assume that the pure states are in the domain of attraction of the limit cycle (41), we can again use the results of section 5.2 to obtain

$$f\left[\frac{\mu - \omega_{1-\nu} t}{p}\right] = f\left[\frac{(1-\omega_\nu)t + 2 + \phi_{1-\nu} - \mu}{p}\right]$$

(where we have fixed the phase of the function $f$ by putting $\phi_\nu \equiv 0$). From this relation we can deduce $\mathrm{d}\phi_\nu/\mathrm{d}\nu = 0$ (by considering $\mu = p$, $t = 0$) and $f[x] = f[(\phi + 2)/p - x]$ (by considering $t = 0$). Finally we arrive at

$$f\left[\frac{\mu - \omega_{1-\nu} t}{p}\right] = f\left[\frac{\mu - (1-\omega_\nu)t}{p}\right] \qquad (\forall\, \mu, t, \nu).$$

If our ansatz is correct and if the corresponding period is the smallest $\Omega$ such that the actual solution can be written in the form (41), we may conclude

$$\omega_{1-\nu} = 1 - \omega_\nu \tag{42}$$

which relates the limit-cycle periods in the upper half of the phase diagram to the periods in the lower half. In particular we have: $\omega_0 = 1$, $\omega_{0.5} = \frac{1}{2}$, $\omega_1 = 0$ (or, in terms of periods: $\Omega_0 = p$, $\Omega_{0.5} = 2p$, $\Omega_1 = \infty$).

In order to calculate $\omega_\nu = p/\Omega_\nu$ explicitly, we will have to insert the ansatz (41) into the dynamic laws (9):

$$f\left[\frac{\mu-\omega t-\omega}{p}\right] = \left\langle \xi_\mu \tanh\left[\beta\sum_\lambda \xi_\lambda\left\{\nu f\left[\frac{\lambda-\omega t}{p}\right]+(1-\nu)f\left[\frac{\lambda-1-\omega t}{p}\right]\right\}\right]\right\rangle_\xi . \tag{43}$$

Since $\mu$ and $t$ can only have discrete values, the problem of calculating $f$ and $\omega$ from (43) is well defined only for large $p$ and upon assuming continuity and continuous differentiability of $f$. Therefore we will restrict ourselves to the large $p$ case and expand (43):

$$f\left[\frac{\mu-\omega t}{p}\right]-\frac{\omega}{p}f'\left[\frac{\mu-\omega t}{p}\right]+\mathcal{O}(p^{-2}) = \left\langle \xi_\mu \tanh\left[\beta\sum_\lambda \xi_\lambda f\left[\frac{\lambda-\omega t}{p}\right]\right]\right\rangle_\xi - \frac{\beta(1-\nu)}{p}\sum_\rho f'\left[\frac{\rho-\omega t}{p}\right] \times\left\langle \xi_\mu\xi_\rho\left\{1-\tanh^2\left[\beta\sum_\lambda \xi_\lambda f\left[\frac{\lambda-\omega t}{p}\right]\right]\right\}\right\rangle_\xi+\cdots .$$

Comparing the lowest orders, and assuming the terms with derivatives of $f$ to contribute increasingly smaller powers of $p$, gives two equations:

$$f\left[\frac{\mu-\omega t}{p}\right] = \left\langle \xi_\mu \tanh\left[\beta\sum_\lambda \xi_\lambda f\left[\frac{\lambda-\omega t}{p}\right]\right]\right\rangle_\xi \tag{44}$$

$$\frac{\omega}{p}f'\left[\frac{\mu-\omega t}{p}\right]+\mathcal{O}(p^{-2}) = \frac{\beta(1-\nu)}{p}\sum_\rho f'\left[\frac{\rho-\omega t}{p}\right] \times\left\langle \xi_\mu\xi_\rho\left\{1-\tanh^2\left[\beta\sum_\lambda \xi_\lambda f\left[\frac{\lambda-\omega t}{p}\right]\right]\right\}\right\rangle_\xi+\cdots . \tag{45}$$

Finally we expand (44) for $t = 1$ in $\omega/p$ and choose in (45) $t = 0$:

$$f\left[\frac{\mu}{p}\right] = \left\langle \xi_\mu \tanh\left[\beta\sum_\lambda \xi_\lambda f\left[\frac{\lambda}{p}\right]\right]\right\rangle_\xi \tag{46}$$

$$f'\left[\frac{\mu}{p}\right]+\mathcal{O}(p^{-1}) = \beta\sum_\rho f'\left[\frac{\rho}{p}\right]\left\langle \xi_\mu\xi_\rho\left\{1-\tanh^2\left[\beta\sum_\lambda \xi_\lambda f\left[\frac{\lambda}{p}\right]\right]\right\}\right\rangle_\xi+\cdots \tag{47}$$

$$\omega f'\left[\frac{\mu}{p}\right]+\mathcal{O}(p^{-1})$$

$$= \beta(1-\nu)\sum_{\rho} f'\left[\frac{\rho}{p}\right]\left\langle \xi_\mu \xi_\rho \left\{1-\tanh^2\left[\beta\sum_{\lambda}\xi_\lambda f\left[\frac{\lambda}{p}\right]\right]\right\}\right\rangle_{\xi} + \cdots . \tag{48}$$

Equation (46) shows that for large $p$ the shape of the periodic ansatz (41) corresponds to that of one of the spurious fixed-points of the Hopfield model. Combining equations (47) and (48) immediately yields the large $p$ expression for the relative sequence velocity $\omega \equiv p/\Omega$:

$$\lim_{p\to\infty} \omega_\nu = 1-\nu. \tag{49}$$

In terms of periods: $\Omega_\nu \to p/(1-\nu)$ for $p \to \infty$. The derivation leading to this result is far from being rigorous; several assumptions on the large $p$ behaviour of the expansion terms of (43) were made (of the type: $q_\mu(t+1)-q_\mu(t) = \mathcal{O}(1/p)$). However, numerical experiments show that expression (49) describes the actual values of the attractor periods surprisingly well, even for relatively small values of $p$. The only restriction is (as might have been expected) that (49) no longer applies if one crosses the first-order transition lines $\nu_\pm(T)$ (where $\omega$ becomes either 0 or 1).

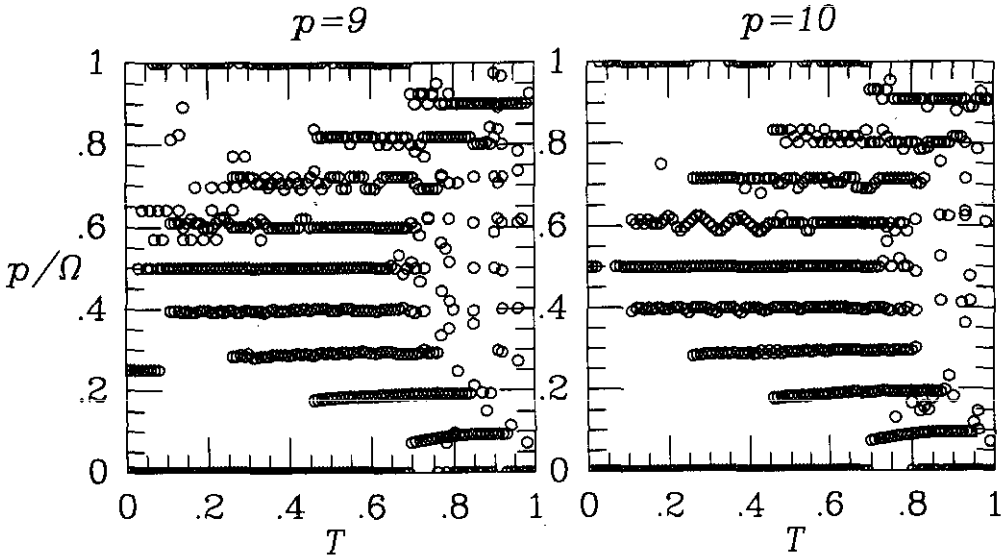


**Figure 9.** The relative sequence processing speed $p/\Omega$ as a function of temperature for $\nu = 0.1$ to 0.9 (top to bottom, $\Delta\nu = 0.1$) and parallel dynamics. Note that equation (49) predicts $p/\Omega = 1-\nu$ in the limit of large $p$.

Figure 9 shows the result of determining the relative sequence speeds $\omega \equiv p/\Omega$ numerically (after iteration of the mappings (9)) for $p = 9$ and $p = 10$, as a function of $T$. The values chosen for $\nu$ ranged between 0.1 and 0.9 ($\Delta\nu = 0.1$). These results show that, away from the first-order transitions, expression (49) holds in good approximation. The only influence of the temperature on $\omega$ (and $\Omega$) seems to be that $T$ determines whether or not the first-order transition lines have been crossed. Once in the middle region of the phase diagram ($\nu_-(T) < \nu < \nu_+(T)$), the attractor periods will depend on $\nu$ only. Taking the effect of the possible crossing of the

transition lines $\nu_{\pm}(T)$ (by variation of $\nu$) into account, one arrives for large $p$ at the relation depicted in figure 10. The positions of the discontinuities depend on $T$ and are given by (40). For finite $p$ one must, in addition, take into account that near $T = 1$ the system might evolve towards the full mixture fixed-point $q^{+}$.

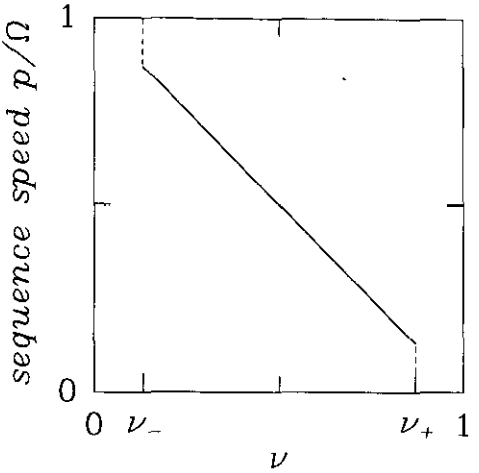


**Figure 10.** The large $p$ relation between the relative sequence processing speed $p/\Omega$ and $\nu$ (parallel dynamics; the temperature dependent locations $\nu_{\pm}$ of the discontinuities are given by the first-order transition lines $\nu_{\pm}(T)$).

## 7. Discussion

In this paper we have studied the competition between pattern reconstruction and sequence processing in an Ising spin model of a neural network in which the interaction matrix is composed of a symmetric Hebbian term and a non-symmetric transition term. For $p = 2$ analysing the model became trivial; due to its periodicity the $p = 2$ transition term is symmetric and we could both solve the dynamics and calulate the free energy.

The behaviour of the $p > 2$ model with parallel dynamics can be described as follows. For each temperature $T < T_c = 1$ there are three regimes in terms of the relative weight $\nu$ of the two terms in the interaction matrix ($\nu = 1$: symmetric term only, $\nu = 0$: transition term only). Near $\nu = 1$ (dominating Hebbian term) the system goes to a fixed-point; the only effect of the presence of the transition term is that this fixed-point will have non-zero correlations with *all* patterns involved. Near $\nu = 0$ (dominating transition term) the system goes to a period-$p$ limit cycle; the only effect of the presence of the Hebbian term is that this limit cycle will have non-zero correlations with *all* patterns involved. In the intermediate region the system either goes to the full mixture fixed-point $q = q(T)(1, \ldots, 1)$ (for $p$ sufficiently small) or to a limit cycle with a period $\Omega$ in between the two extreme cases: $\Omega \in [p, \infty]$. For large $p$ we have derived an asymptotic expression for this period; numerical iteration of the dynamic equations shows this expression to hold in good approximation already for $p \sim 10$. The transitions between the three regions are first order. In the limit $p \to \infty$ the full mixture fixed-point will eventually become unstable for all $\nu$,

$T < 1$. It turned out that all dynamic solutions of the macroscopic laws for the order parameters (overlaps) in the region $\nu > \frac{1}{2}$ are related to the solutions in the region $\nu < \frac{1}{2}$ by a time-dependent unitary transformation, which explains the symmetry of the phase diagrams.

The behaviour of the $p > 2$ model with sequential dynamics is different. Near $\nu = 1$ (dominating Hebbian term) the system again goes to a fixed-point which has non-zero correlations with *all* patterns involved. If $\nu$ is lowered (increasing importance of the transition term) a first-order transition occurs and the system either goes to the full mixture fixed-point $q = q(T)(1, \ldots, 1)$ (for $p$ sufficiently small) or to a limit cycle (for $p$ sufficiently large). In the limit $p \to \infty$ the full mixture fixed-point will again eventually become unstable for all $\nu$, $T < 1$. In contrast to the previous situation, there is no symmetry in the phase diagram corresponding to the interchange of the Hebbian term and the transition term; accordingly there is no evidence for a second first-order transition in the region $\nu < \frac{1}{2}$. An interesting result is the very presence (for $p$ sufficiently large) of stable non-stationary limit cycles; intuitively one would expect that without stabilizing mechanisms sequential dynamics would always drive the system towards the full mixture fixed-point.

If we compare our results with those obtained in [11] and [12] for the symmetric version of the present model, the most important difference (apart from the presence of stable non-stationary trajectories) is the absence in the present model of zero temperature $\nu < \frac{1}{2}$ fixed-points with a finite number of non-zero components. At $T = 0$ we find that there are pure fixed points for $\nu > \frac{1}{2}$ and only fully symmetric fixed-points for $\nu < \frac{1}{2}$. Fixed-points of the type encountered in the experiments of Miyashita [13] are found only for $0 < T < 2\nu - 1$; these fixed-points have non-zero components only (although only two or three components turn out to be noticably non-zero).

In spite of the non-symmetry of the interaction matrix it turned out that it still contained enough structure to enable us to build a comprehensive picture of the system's phase diagram. The two most important building blocks for our analysis are (a) the fact that in all of the region $T > 2\nu - 1$ we could prove all possible fixed-points to be symmetric in the pattern index (whatever choice of dynamics); and (b) the duality between the dynamic solutions for parallel dynamics with respect to interchanging the relative weights of the two terms in the interaction matrix (caused by symmetries in the dynamical laws for the evolution of the order parameters). If we examine more closely the statistical properties of the stored patterns (in this paper the patterns were chosen to be drawn at random) that were really essential for our analysis, it turns out that the only requirement for being able to generalise our calculations to the case of more general definitions of patterns is that the pattern correlation matrix $C$ must commute with $S$, and therefore must be a Toeplitz matrix, i.e. $C_{\mu\nu} = g(\mu - \nu)$ (for some periodic function $g$). This means that as a next step we might analyse the behaviour of the present model for those situations where subsequent patterns are correlated (which will be the subject of a future paper).

## 8. Appendix: uniqueness of the fixed-point

In this section we show that for $T > 2\nu - 1$ any fixed point $q \neq \mathbf{0}$ of the fixed-point equation (16) must have the property: $q_\lambda = q_\mu$ for all $\lambda$ and $\mu$. This immediately leads to the conclusion that the only non-trivial fixed points are $\pm q^+$. Suppose that

two real-valued $p$-dimensional vectors $q$ and $k$ are related by

$$q = \langle \xi \tanh(\beta \xi \cdot k) \rangle_\xi$$

where (as throughout the paper) the vectors $\xi$ are drawn from the set $\{-1, 1\}^p$ with uniform probabilities, then the following identities hold:

$$q_\mu - q_\lambda = \left\langle \tanh\left[\beta(k_\mu - k_\lambda) + \beta \sum_{\rho \neq \mu,\lambda} \xi_\rho k_\rho\right] \right\rangle_\xi . \tag{50}$$

For $T > 0$ these enable us to conclude

$$\operatorname{sgn}(q_\mu - q_\lambda) = \operatorname{sgn}(k_\mu - k_\lambda) \qquad \forall \mu, \lambda$$
$$|q_\mu - q_\lambda| \leqslant \tanh(\beta |k_\mu - k_\lambda|) \leqslant \beta |k_\mu - k_\lambda| \qquad \forall \mu, \lambda .$$

In our case the fixed-point equation (16) is obtained by making the identification $k \equiv Aq$, which yields

$$\operatorname{sgn}(q_\mu - q_\lambda) = \operatorname{sgn}\left((Aq)_\mu - (Aq)_\lambda\right) \qquad \forall \mu, \lambda$$
$$|q_\mu - q_\lambda| \leqslant \tanh(\beta |(Aq)_\mu - (Aq)_\lambda|) \leqslant \beta |(Aq)_\mu - (Aq)_\lambda| \qquad \forall \mu, \lambda .$$

From these relations one can derive many conclusions on the dependence of the possible fixed-points on properties of the matrix $A$. For the Hopfield model [2] ($A = 1$) these relations are empty statements; however, in general they turn out to be rather restrictive. Here we will proceed by making for $A$ the choice $A = \nu + (1-\nu)S$ (with $\nu < 1$), with the result

$$\operatorname{sgn}(q_\mu - q_\lambda) = \operatorname{sgn}\left[\nu(q_\mu - q_\lambda) + (1-\nu)(q_{\mu-1} - q_{\lambda-1})\right] \qquad \forall \mu, \lambda \pmod p$$
$$|q_\mu - q_\lambda| \leqslant \beta |\nu(q_\mu - q_\lambda) + (1-\nu)(q_{\mu-1} - q_{\lambda-1})| \qquad \forall \mu, \lambda \pmod p .$$

From these relations, in turn, it follows that for all $\lambda, \mu \pmod p$:

$$q_\lambda = q_\mu \text{ or } (q_\mu - q_\lambda)(q_\mu - q_\lambda + q_{\mu-1} - q_{\lambda-1}) \geqslant \frac{T - 2\nu + 1}{1 - \nu}(q_\mu - q_\lambda)^2 > 0 . \tag{51}$$

For $T = 0$ we can also arrive at (51); in this case it follows from (50) that

$$(q_\mu - q_\lambda)(k_\mu - k_\lambda) \geqslant 0 .$$

Insertion of $k = Aq$ with $A \equiv \nu + (1-\nu)S$ gives immediately the $T = 0$ version of (51). Therefore (51) holds for all $T > 2\nu - 1$.

Relations (51) turn out to be sufficient for proving that $q_\mu = q_\lambda$ for all $\lambda, \mu$ (the following version of the remaining proof we owe to David Rabson). Suppose that the components of $q$ are *not* all the same. It then follows that an index $\rho$ exists, such that

$$q_\rho \leqslant q_\lambda \ (\forall \lambda) \qquad q_{\rho+1} > q_\rho .$$

We can now proceed by induction: if for any given $n \geqslant 0$ we know that $q_{\rho+1} > q_{\rho-n}$, then upon choosing $\mu \equiv \rho + 1$ and $\lambda \equiv \rho - n$ equation (51) tells us that

$$q_{\rho+1} + q_\rho > q_{\rho-n} + q_{\rho-n-1}$$

so

$$q_{\rho+1} > q_{\rho-n-1} + q_{\rho-n} - q_\rho \geqslant q_{\rho-n-1}.$$

Repeating the argument shows that the propositions $q_{\rho+1} > q_\rho$ and $q_\rho \leqslant q_\lambda \forall \lambda$ will inevitably lead to the contradiction $q_{\rho+1} > q_{\rho+1}$. The final conclusion must be that if $T > 2\nu - 1$ then all components $q_\mu$ of a solution $q$ of the fixed-point equation (16) must be equal; therefore the only non-trivial fixed-points are $q = \pm q^+$.

## References


[1] Little W A 1974 *Math. Biosci.* **19** 101
[2] Hopfield J J 1982 *Proc. Natl Acad. Sci., USA* **79** 2554
[3] Amit D J, Gutfreund H and Sompolinsky H 1985 *Phys. Rev.* A **32** 1007
[4] Coolen A C C and Ruijgrok Th W 1988 *Phys. Rev.* A **38** 4253
[5] Hebb D O 1949 *The Organization of Behaviour* (New York: Wiley)
[6] Dotsenko V S, Yarunin N D and Dorotheyev E A 1991 *J. Phys. A: Math. Gen.* **24** 2419
Dotsenko V S and Tirozzi B 1991 *J. Phys. A: Math. Gen.* **24** 5163
[7] Kohonen T O 1984 *Self-organization and Associative Memory* (Berlin: Springer)
[8] Evans M R, Wallace D J and Zhan C 1991 *J. Phys. A: Math. Gen.* **24** 4445
[9] Coolen A C C, Noest A J and de Vries G B 1992 *Preprint OUTP-92-28S* University of Oxford
[10] Coolen A C C and Noest A J 1990 *J. Phys. A: Math. Gen.* **23** 575
[11] Griniasty M, Tsodyks M V and Amit D J 1992 *Preprint* Universita di Roma 'La Sapienza' N856
[12] Cugliandolo L F 1992 *Preprint* Universita di Roma 'La Sapienza'
[13] Miyashita Y and Chang H S 1988 *Nature* **331** 68
Miyashita Y 1988 *Nature* **335** 817
Sakai K and Miyashita Y 1991 *Nature* **354** 152
[14] Kühn R and van Hemmen J L 1991 *Models of Neural Networks* (Berlin: Springer)
[15] Sompolinsky H and Kanter I 1986 *Phys. Rev. Lett.* **57** 2861
[16] Herz A V M, Li Z and van Hemmen J L 1991 *Phys. Rev. Lett.* **66** 1370
[17] Bauer K and Krey U 1991 *Z. Phys.* B **84** 131
[18] Mato G and Parga N 1991 *Z. Phys.* B **84** 483
[19] Coolen A C C 1990 *Statistical Mechanics of Neural Networks* (Berlin: Springer)
Coolen A C C and Lenders L G V M 1992 *J. Phys. A: Math. Gen.* **25** 2577
[20] Bernier O 1991 *Europhys. Lett.* **16** 531
[21] Peretto P 1984 *Biol. Cybern.* **50** 51
[22] Nishimori H, Nakamura T and Shiino M 1990 *Phys. Rev.* A **41** 3346